Supporting Information

iClick Synthesis of Network Organometallic Polymers

Yu-Hsuan Shen,[a] Ion Ghiviriga,[a] Khalil A. Abboud,[a] Kirk S. Schanze,[b] Adam S. Veige.*[a]

a. University of Florida, Department of Chemistry, Center for Catalysis, P.O. Box 117200, Gainesville, FL, 32611.
b. University of Texas at San Antonio, Department of Chemistry, One UTSA Circle, San Antonio, TX 78249.

Corresponding Authors

* E-mail: veige@chem.ufl.edu

Table of Contents

1. Syntheses, NMR and X-ray Crystallography Data

1.1 General Considerations

Materials:

All manipulations were set up under an inert atmosphere using standard Schlenk or glove-box techniques for convenience; however, the compounds are isolated using benchtop technique and are stable in air. Pentane, dichloromethane (CH_2Cl_2), and tetrahydrofuran (THF) were degassed by sparging with high purity argon and were dried using a GlassContour drying column. Methanol was dried over anhydrous copper(II) sulfate, distilled and stored over 4 Å molecular sieves; chloroform-*d* (Cambridge Isotopes) was dried over calcium hydride, distilled, and stored over 4 Å molecular sieves.

The following were prepared by literature methods: [Au(N_3)(PPh_3)] (**1-AuN$_3$**),[1] $(AuCl)_2(PPh_2(C_6H_4)PPh_2)$,[2] tetrakis(4-((trimethylsilyl)ethynyl)phenyl)methane,[3] tetrakis(4-ethynylphenyl)methane (**4-H**),[3] 1,3,5-triethynylbenzene (**3-H**),[4] 1,3,5-tris(trimethylsilylethynyl)benzene,[4] 1,3,5-$C_6H_3(C{\equiv}CAu(PPh_3))_3$ (**3-AuPPh$_3$**).[5]

Caution! *Azides and azido complexes are potentially explosive. Reactions should be performed only on a small scale and avoiding heat until stability can be verified.*

Analytical techniques:

NMR spectra were recorded on Bruker Ascend HD III 400 and 600 MHz spectrometers. The spectra were recorded at 25 °C unless noted otherwise. Chemical shifts are reported in δ (ppm). $^{31}P\{^1H\}$ spectra were referenced to an 85% phosphoric acid external standard (0 ppm).

Electrospray ionization mass spectrometry (ESI-MS) spectra were collected by direct injection into an Agilent 6230 Time-of-Flight (TOF) spectrometer at a gas temperature of 350 °C. Matrix assisted laser desorption ionization (MALDI) was

collect by injection into a Bruker autoflex MALDI TOF using reflectron (900-4500 Da) positive mode. Samples were prepared in DCM at 5 mg/mL, dithranol was used as matrix and was dissolved in DCM at 5 mg/mL. Solutions for analysis were prepared by mixing the sample and matrix at a volume ration of 1:1. The sample was left to air dry after spotting on a stainless steel MALDI target plate. The resulting spectra were analyzed using the MassLynx 4.0 software package.

X-Ray intensity data were collected at 100 K on a Bruker Dual micro source D8 Venture diffractometer using Mo Kα radiation (λ = 0.71073 Å) and the crystal structures were refined using full-matrix least-squares refinement.[6] Powder X-ray Diffraction (PXRD) samples were loaded on flat lass slide and data was collected using a Panalytical X'Pert Powder X-ray Diffractometer with Cu Kα radiation (λ = 1.5406 Å) with a scan step size of 0.002° in the 2-theta range of 5-70° under ambient conditions.

Infrared spectra were collected on a Thermo Nicolet 5700 Fourier-transform infrared (FTIR) spectrometer equipped with a single bounce, diamond-stage attenuated total reflectance (ATR) accessory. Elemental analyses were performed at the CENTC Elemental Analysis Facility, Department of Chemistry, University of Rochester and their compositions were determined with a PerkinElmer 2400 Series II Analyzer. Thermogravimetric analyses (TGA) were measured under nitrogen with a TGA Q5000 (TA Instruments). About 10-15 mg of each sample was dried under dynamic vacuum for 24 h, then 5 mg portions of these samples were heated at 20 °C/min from 25 to 600 °C. Differential scanning calorimetry (DSC) thermograms were obtained with a DSC Q1000 (TA instruments). Typically, 4-6 mg of a sample was added to a sealed pan to heat at 5 °C/min. The temperature ranged from -70 to 220 °C.

^{13}C cross-polarization, magic-angle spinning (CPMAS) nuclear magnetic resonance spectra experiments were carried out on a Bruker 600 MHz Avance Neo spectrometer equipped with a 4 mm Bruker HCN biosolids probe. Samples were packed into zirconia rotors with Kel-F drive caps. ^{13}C (150.08 MHz) NMR spectra were collected using ^{1}H - ^{13}C Cross Polarization (CP) at 25 °C at a MAS rate of 13

kHz. CP was accomplished with a 2 μs ^{1}H π/2 pulse followed by 1.6-ms ramped CP with a constant 62.5 kHz ^{13}C RF field. ^{1}H (600.76 MHz) decoupling of 100 kHz was employed during 30-ms of signal acquisition. ^{13}C spectra were referenced externally with adamantane by setting the downfield resonance to 38.48 ppm.

All nitrogen and CO_2 adsorption and desorption isotherms were measured using a Quantachrome ASiQsorb iQ3 and ASiQwin system. Between 50-125 mg of samples were employed in each measurement and the samples were outgassed at 110 °C for 12 h under high vacuum. A test for the rate of rise pressure when vacuum valves are closed was employed at the end of outgas process, the samples would remain outgas until the pressure rate change reached below 20 mtorr/min. Nitrogen adsorption and desorption measurements were done at 77 K. Specific surface areas were calculated from adsorption data using Brunauer-Emmett-Teller (BET) methods in the range of $0.01 < P/P_0 < 0.05$. CO_2 adsorption and desorption measurements were analysis at 273 K, and 298 K.

Transmission electron microscopy (TEM) images were acquired on a FEI TALOS F200I field emission gun scanning/transmission electron microscope. The TEM images were collected at 200 kV voltage and 1.5 nA current with a 0.34 nm point-to-point resolution in conventional TEM imaging. The scanning transmission electron microscopy (STEM) images were operated on the same instrument with a STEM resolution of 136 pm at 200 kV voltage and 20 pA current. Energy-dispersive X-ray spectroscopies (EDS) were collected using Bruker XFlash 6T|30 windowless silicon drift detector (30 square mm detector area) system. Scanning electron microscopy (SEM) and backscattered electron scanning electron microscopy (BSE SEM) images were collected using a FEI Helios G4 PFIB CXe DualBeam system operated at 2 kV voltage and 25 pA current. Samples were prepared by sonicating with methanol for 10 min then carefully dispense on the TEM grid for all microscopy analysis.

1.2 Synthesis of **2-AuN$_3$**

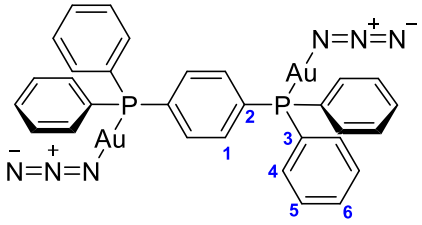

$(AuCl)_2(PPh_2(C_6H_4)PPh_2)$ (182.2 mg, 0.2000 mmol) and silver triflate (51.4 mg, 0.200 mmol), were added into 5 mL of THF and stirred for 5 h. The solution was filter and NaN_3 (100.0 mg, 1.538 mmol) was added into the mixture with THF:MeOH (3:1 v/v, 12 mL) and stirred at room temperature in the absent of light. After 24 h, the solution was poured in 120 mL of CH_2Cl_2 and washed with water 3x. The organic layer was collected and dried over $MgSO_4$. The colorless solution was then removed in vacuo, and the precipitate was collected to give a white powder. Crystals were grown through pentane diffusion into a CH_2Cl_2 solution of **2-AuN$_3$** at -25 °C. 81% Yield (150.7 mg, 0.1629 mmol). ^{1}H NMR (400 MHz, $CDCl_3$): δ 7.64-7.49 (m, 24 H). $^{13}C\{^1H\}$ NMR (101 MHz, $CDCl_3$)): δ 134.4 (d, $^2J_{CP}$ = 14 Hz, C_4), 134.0 (t, $^2J_{CP}$ = 13 Hz, C_1), 133.4 (d, $^1J_{CP}$ = 2 Hz, C_2), 132.6 (m, C_6), 129.6 (d, $^3J_{CP}$ = 12 Hz, C_5),127.2 (d, $^1J_{CP}$ = 63 Hz, C_3). $^{31}P\{^1H\}$ NMR (162 MHz, $CDCl_3$): δ 30.9. FTIR (cm^{-1}): 2965 (m), 2918 (m), 2852 (m), 2052 (vs, azide stretch), 1719 (m), 1434 (s), 1272 (m), 1099 (m), 871 (m). Anal. Calcd. for $C_{30}H_{24}Au_2N_6P_2$: C, 38.98; H, 2.62; N, 9.09. Found: C, 38.75; H, 2.60; N, 8.00.

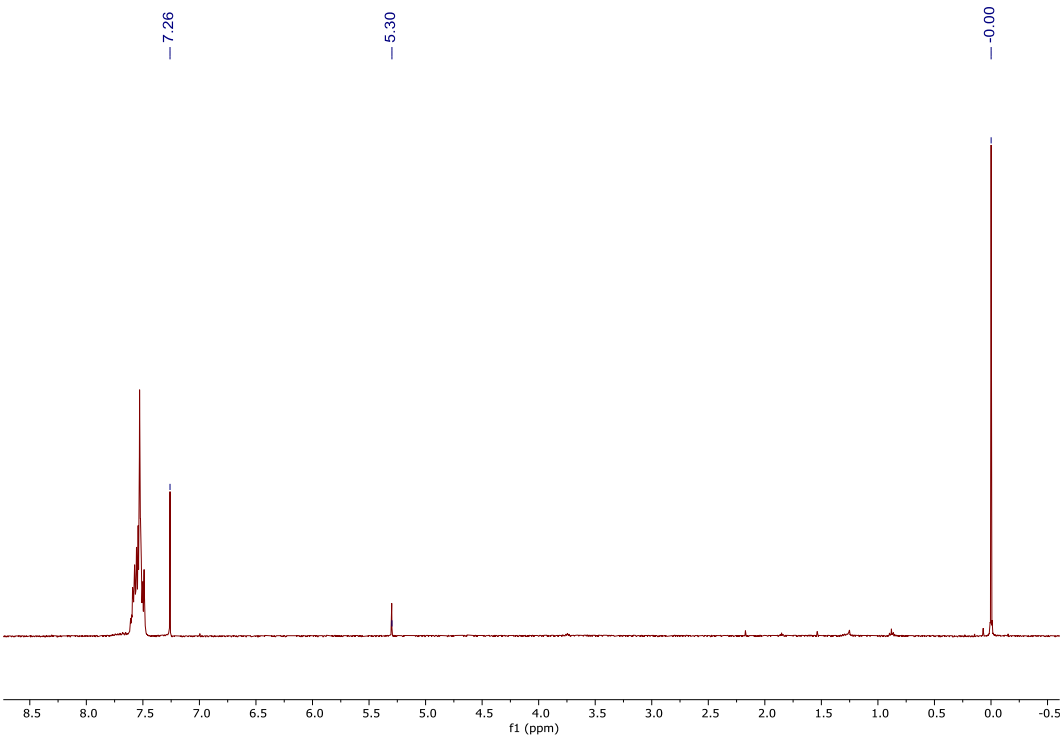

Figure S1. ^{1}H NMR spectrum of **2-AuN$_3$** ($CDCl_3$, 400 MHz).

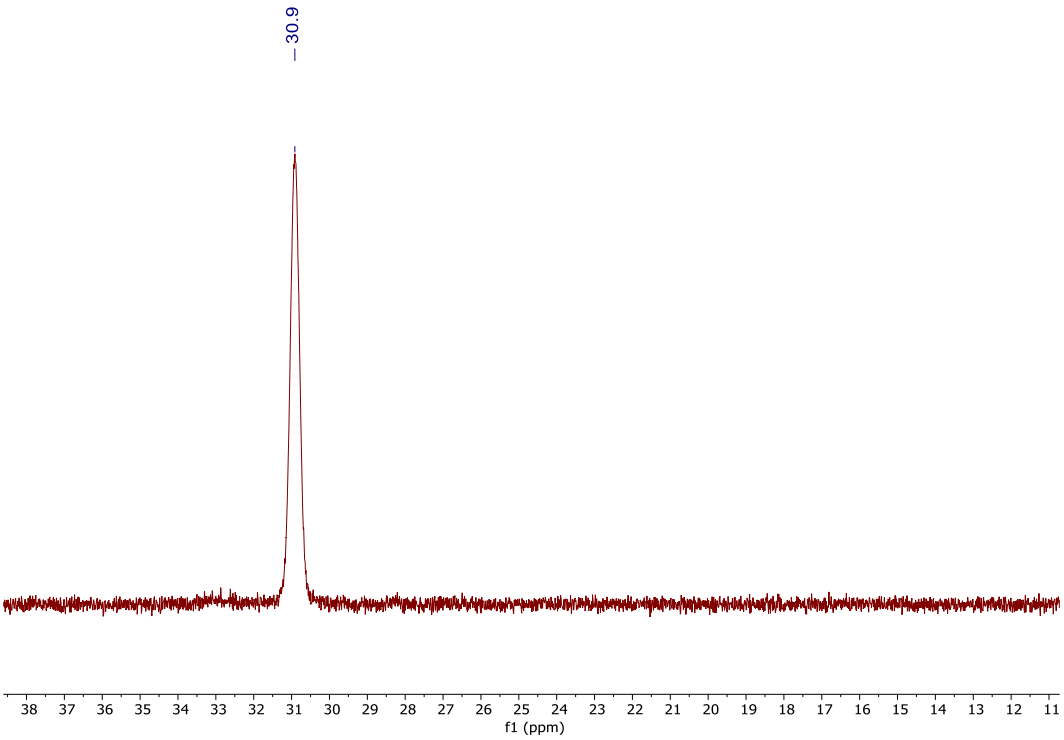

Figure S2. $^{31}P\{^{1}H\}$ NMR spectrum of **2-AuN$_3$** ($CDCl_3$, 162 MHz).

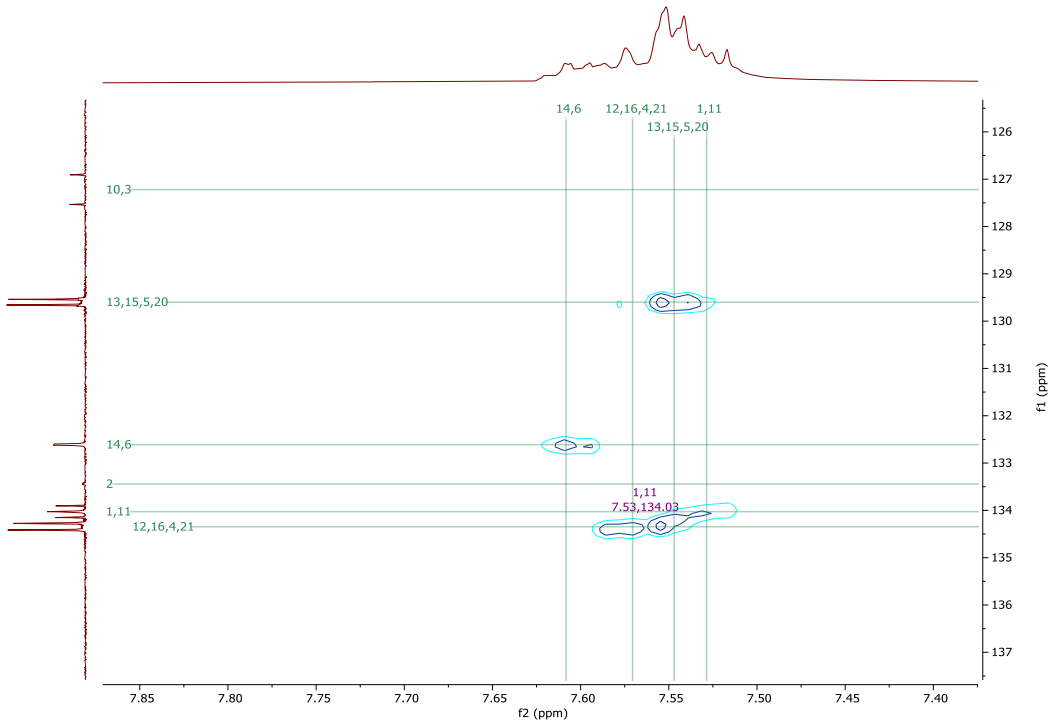

Figure S3. ^{1}H-^{13}C gHSQC spectrum of **2-AuN$_3$** ($CDCl_3$, 400 MHz).

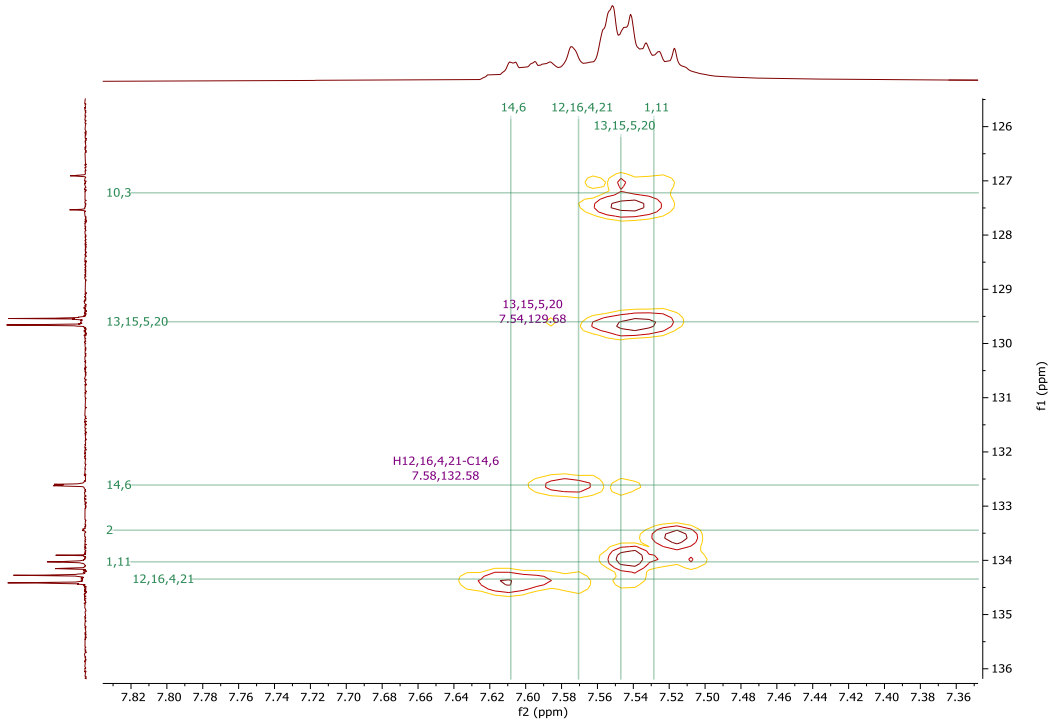

Figure S4. ^{1}H-^{13}C gHMBC spectrum of **2-AuN$_3$** ($CDCl_3$, 400 MHz).

1.3 X-Ray Crystallography of **2-AuN$_3$**

X-Ray Intensity data were collected at 100 K on a Bruker Dual micro source D8 Venture diffractometer and PHOTON III detector running APEX3 software package of programs and using Mo Kα radiation (λ = 0.71073 Å). The data frames were integrated, and multi-scan scaling was applied in APEX3. Intrinsic phasing structure solution provided all of the non-H atoms.

The structure was refined using full-matrix least-squares refinement.[6] The non-H atoms were refined with anisotropic displacement parameters and all of the H atoms were calculated in idealized positions and refined riding on their parent atoms. The azide groups were disordered and refined in two parts with their site occupation factors dependently refined. In the final cycle of refinement, 4885 reflections (of which 4287 are observed with I > 2 σ (I)) were used to refine 179 parameters and the resulting R_1, wR_2 and S (goodness of fit) were 2.94%, 6.92% and 1.209, respectively. The refinement was carried out by minimizing the wR_2 function using F^2 rather than F values. R_1 is calculated to provide a reference to the conventional R value but its function is not minimized.

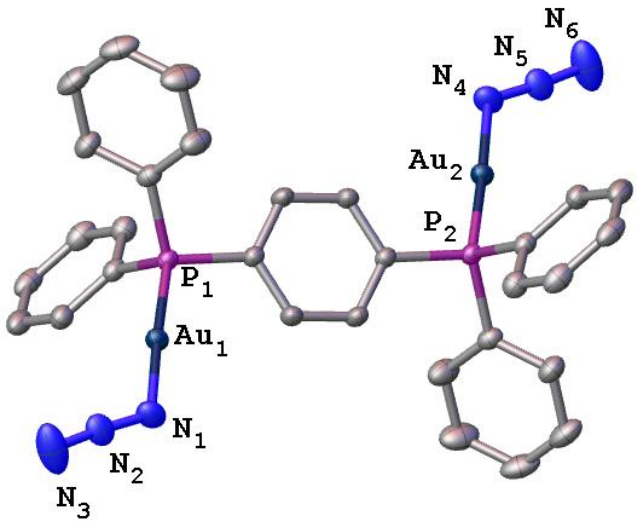

Figure S5. Molecular structure of **2-AuN$_3$** (Hydrogen atoms removed for clarity).

Table S1. Crystal data and structure refinement for **2-AuN_3**.

CCDC Number	**2158225**
Empirical formula	$C_{30}H_{24}Au_2N_6P_2$
Formula weight	924.42
Temperature	100(2) K
Wavelength	0.71073 Å
Crystal system	Monoclinic
Space group	*C2/c*
Unit cell dimensions	*a* = 17.3378(7) Å, *α*= 90°. *b* = 13.2670(5) Å, *β*= 97.1990(10)°. *c* = 12.2141(4) Å, *γ*= 90°.
Volume	2787.35(18) $Å^3$
Z	4
Density (calculated)	2.203 Mg/m^3
Absorption coefficient	10.662 mm^{-1}
F(000)	1736
Crystal size	0.200 x 0.090 x 0.060 mm^3
Theta range for data collection	1.939 to 33.208°.
Index ranges	-25≤h≤26, -20≤k≤20, -18≤l≤14
Reflections collected	40363
Independent reflections	4885 [R(int) = 0.0437]
Completeness to theta = 25.242°	98.3 %
Absorption correction	none
Refinement method	Full-matrix least-squares on F^2
Data / restraints / parameters	4885 / 0 / 179
Goodness-of-fit on F^2	1.209
Final R indices [I>2sigma(I)]	R_1 = 0.0294, wR_2 = 0.0692 [4287]
R indices (all data)	R_1 = 0.0338, wR_2 = 0.0711
Extinction coefficient	n/a
Largest diff. peak and hole	1.686 and -3.371 $e.Å^{-3}$

1.4 Synthesis of **3-AuPEt$_3$**

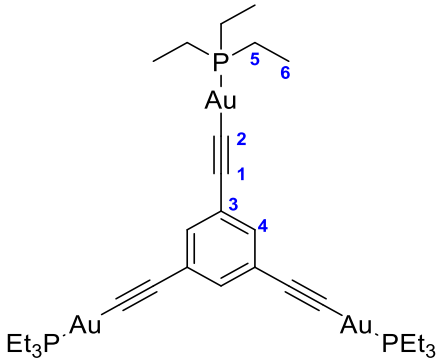

Complex **3-AuPEt$_3$** was synthesized using a slightly modified procedure from the literature reported 1,3,5-$C_6H_3(C{\equiv}CAu(PPh_3))_3$ (**3-AuPPh$_3$**)[5] synthesis. $AuCl(PEt_3)$ (420.9 mg, 1.200 mmol), 1,3,5-triethynylbenzene (134.6 mg, 0.400 mmol), and sodium methoxide (25 wt. % in methanol, 1 mL) were added into a mixture of THF:MeOH (2:1 v/v, 6 mL). The reaction mixture was stirred at room temperature for 24 h then poured in 200 mL of CH_2Cl_2. The solution was washed with water 3x, dried over $MgSO_4$, filtered, and removed then all volatiles were removed in vacuo. The resulting powder was further washed with toluene to obtain **3-AuPEt$_3$** as a yellow solid. 81% Yield (0.3236 mmol, 353.5 mg). ^{1}H NMR (400 MHz, $CDCl_3$): δ 7.44 (s, 3H, C_4-H), 1.80 (m, 18H, C_5-H), 1.20 (3, 27H, C_6-H). $^{13}C\{^1H\}$ NMR (101 MHz, $CDCl_3$)): δ 134.7 (d, $^2J_{CP}$ = 140 Hz, C_2), 134.7 (s, C_4), 124.5 (s, C_3), 103.3 (d, $^3J_{CP}$ = 27 Hz, C_1), 17.8 (d, $^2J_{CP}$ = 33 Hz, C_5), 8.9 (s, C_6). $^{31}P\{^1H\}$ NMR (162 MHz, $CDCl_3$): δ 37.7. FTIR (cm^{-1}): 2962 (m), 2929 (m), 2827 (m), 2100 (w; alkyne strech), 1565 (m), 1452 (m), 1413 (m), 1039 (m), 965 (m), 870 (m). MALDI-TOF-MS: m/z calculated for $C_{30}H_{48}Au_3P_3$ $[M+H]^+$ 1093.2039, found 1093.0107.

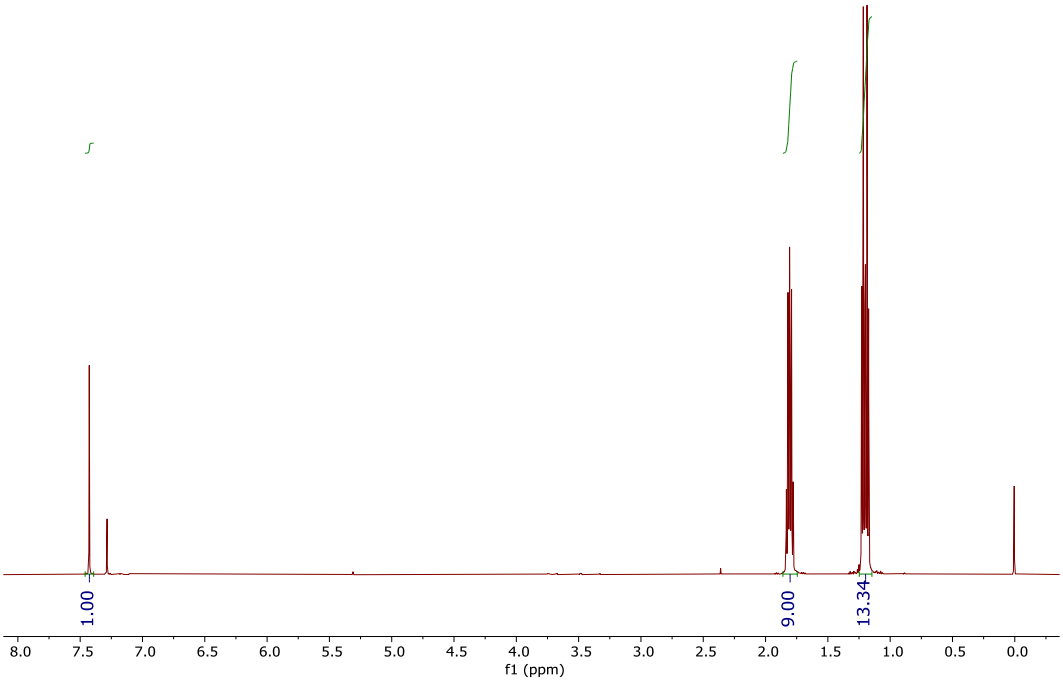

Figure S6. ^{1}H NMR spectrum of **3-AuPEt$_3$** ($CDCl_3$, 400 MHz).

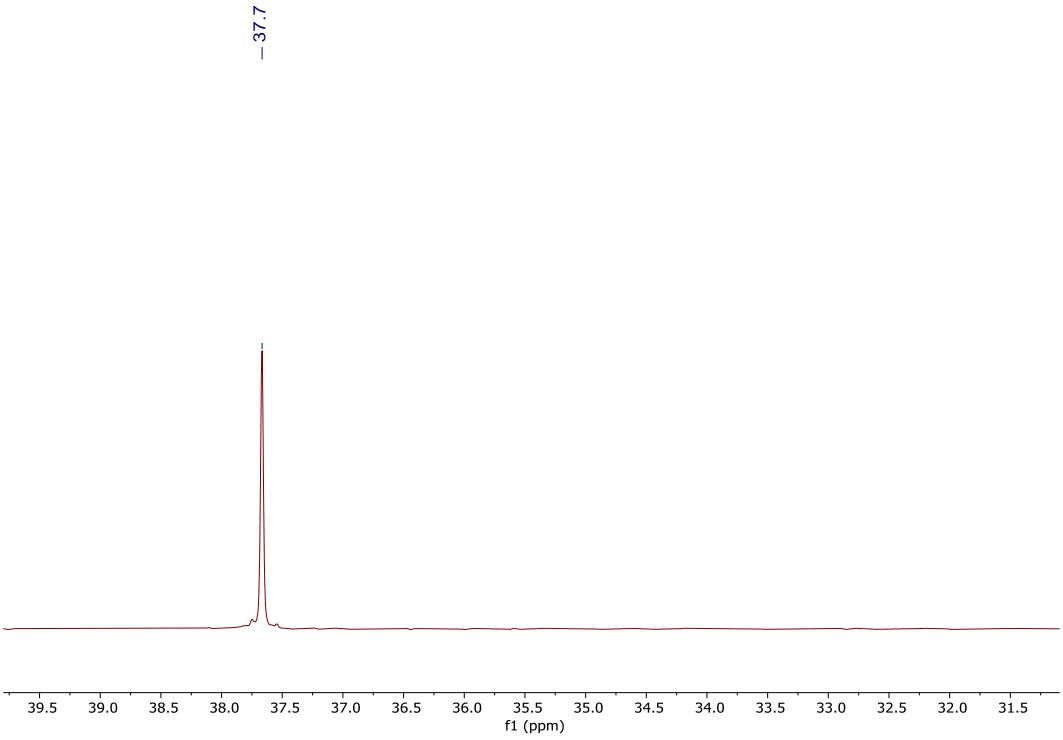

Figure S7. $^{31}P\{^{1}H\}$ NMR spectrum of **3-AuPEt$_3$** ($CDCl_3$, 162 MHz).

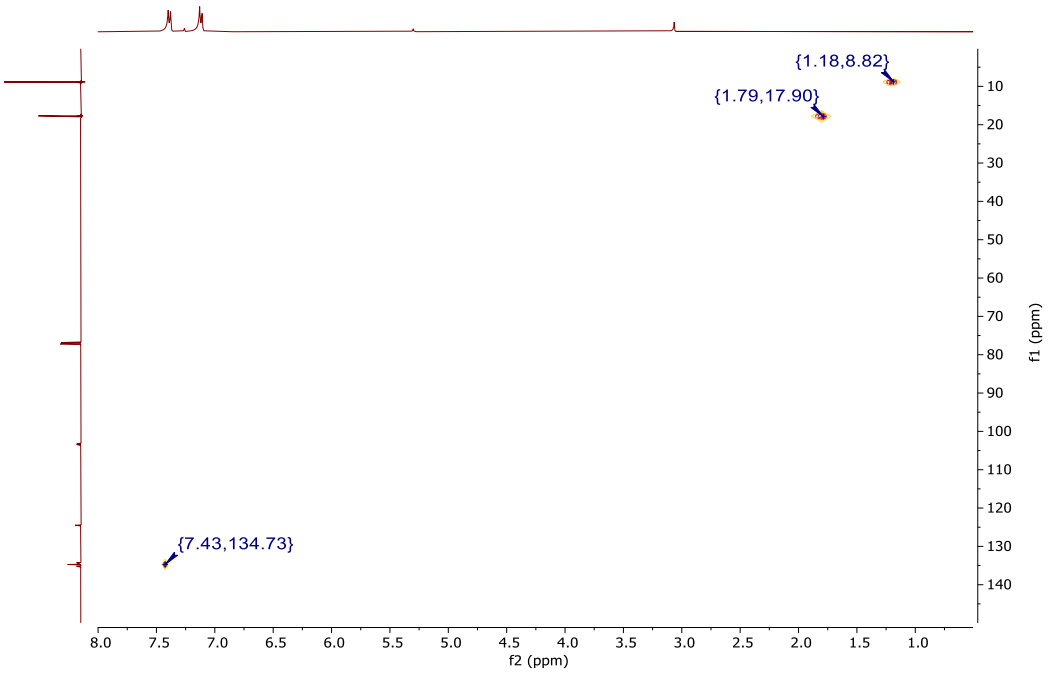

Figure S8. ^{1}H-^{13}C gHSQC spectrum of **3-AuPEt$_3$** ($CDCl_3$, 400 MHz).

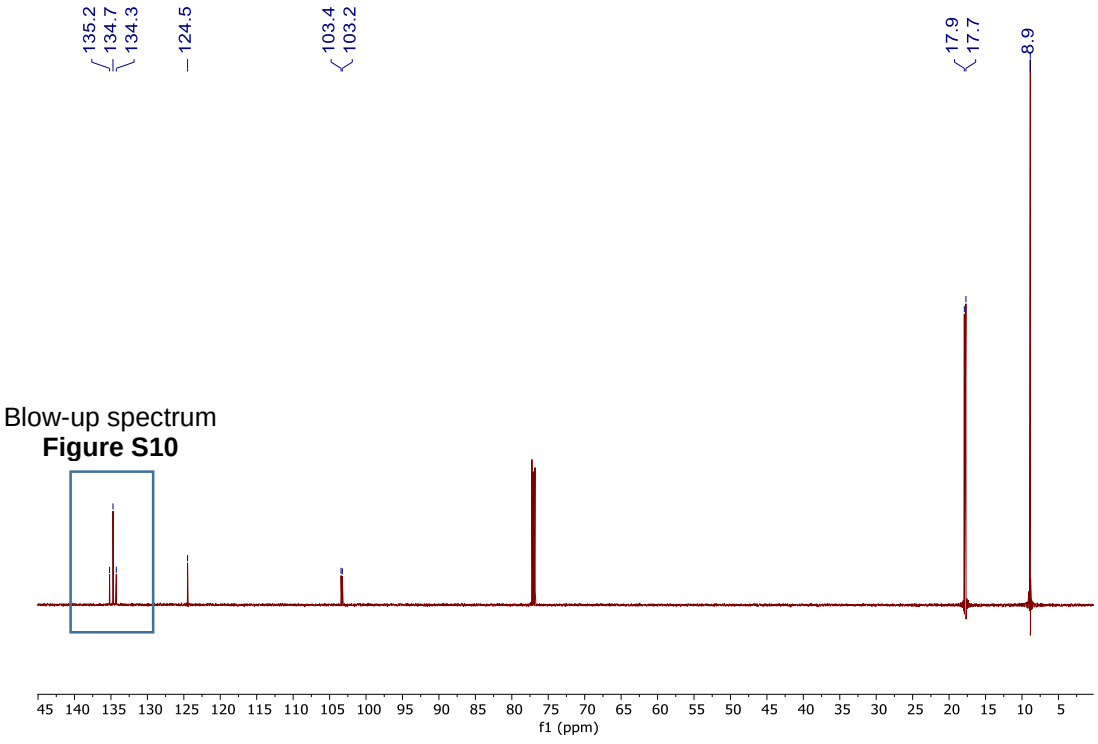

Blow-up spectrum
Figure S10

Figure S9. ^{13}C spectrum of **3-AuPEt$_3$** ($CDCl_3$, 101 MHz).

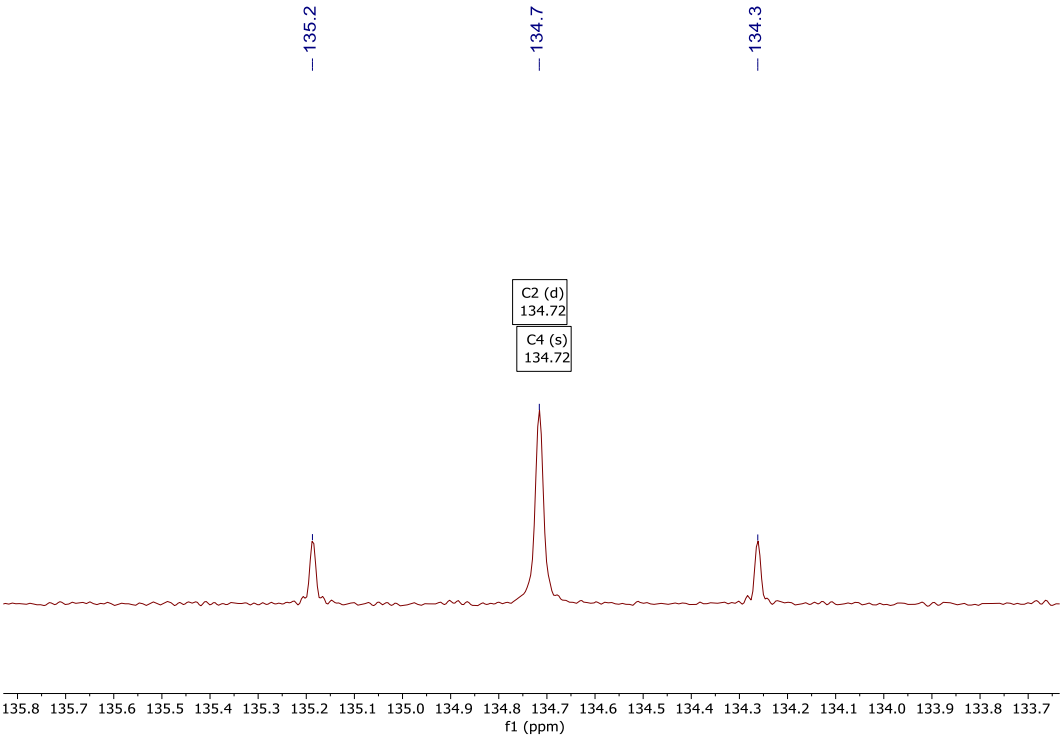

Figure S10. Blow-up ^{13}C spectrum of **3-AuPEt$_3$** from 133.7-135.7 ppm ($CDCl_3$, 101 MHz).

1.5 Synthesis of **4-AuPPh$_3$**

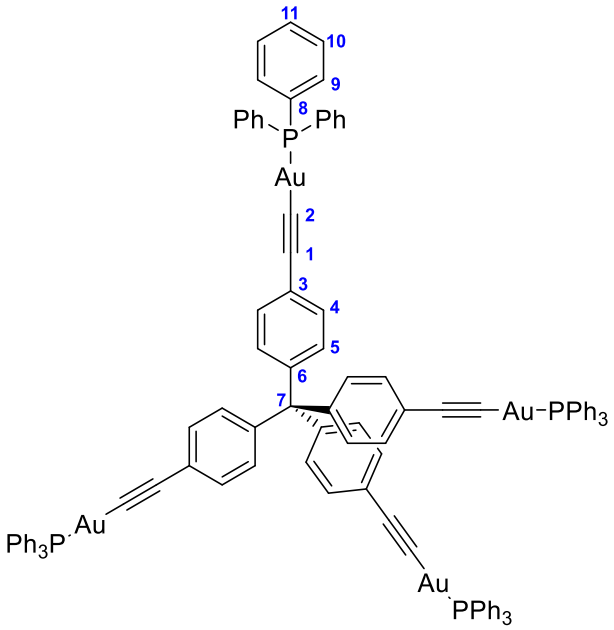

Tetrakis(4-((trimethylsilyl)ethynyl)phenyl)methane (141.1 mg, 0.2000 mmol), AuCl(PPh$_3$) (396.2 mg, 0.8008 mmol), and sodium methoxide (25 wt. % in methanol, 1 mL) were added into a mixture of THF:MeOH (2:1 v/v, 6 mL). The reaction mixture was stirred at room temperature for 24 h then poured into 200 mL of CH_2Cl_2. The solution was washed with water 3x, dried over $MgSO_4$, filtered, and then all volatiles were removed in vacuo. The powder was further washed with toluene to obtain **4-AuPPh$_3$** as a yellow solid. Crystals were grown through pentane diffusion into a CH_2Cl_2 solution of **4-AuPPh$_3$** at -25 °C. 71% Yield (0.1424 mmol, 320.5 mg). ^{1}H NMR (400 MHz, $CDCl_3$): δ 7.59-7.39 (m, 60H, C_9-H, C_{10}-H and C_{11}-H), 7.36 (d, $^3J_{HH}$ = 8.7 Hz, 8H, C_4-H), 7.00 (d, $^3J_{HH}$ = 8.7 Hz, 8H, C_5-H). ^{13}C{^{1}H} NMR (101 MHz, $CDCl_3$)): δ 145.0 (s, C_6), 134.3 (d, $^2J_{CP}$ = 14 Hz, C_9), 131.5 (d, $^4J_{CP}$ = 2 Hz, C_{11}), 131.3 (s, C_4), 130.8 (s, C_5), 129.8 (d, $^1J_{CP}$ = 56 Hz, C_8), 129.1 (d, $^3J_{CP}$ = 11 Hz, C_{10}), 122.4 (d, $^4J_{CP}$ = 3 Hz, C_3), 104.0 (d, $^3J_{CP}$ = 27 Hz, C_1), 64.4 (C_7). ^{31}P{^{1}H} NMR (162 MHz, $CDCl_3$): δ 42.3. FTIR (cm^{-1}): 3058 (m), 2984 (m), 2862 (m), 2119 (w; alkyne stretch), 1501 (m), 1435 (m), 1186 (w), 1099 (m), 1066 (m), 830 (m). Anal. Calcd. for $C_{105}H_{76}Au_4P_4$: C, 56.06; H, 3.41. Found: C, 56.58; H, 3.46; N, 0.03. MALDI-TOF-MS: m/z calculated for $C_{105}H_{76}Au_4P_4$ $[M+H]^+$ 2250.3667, found 2250.0669.

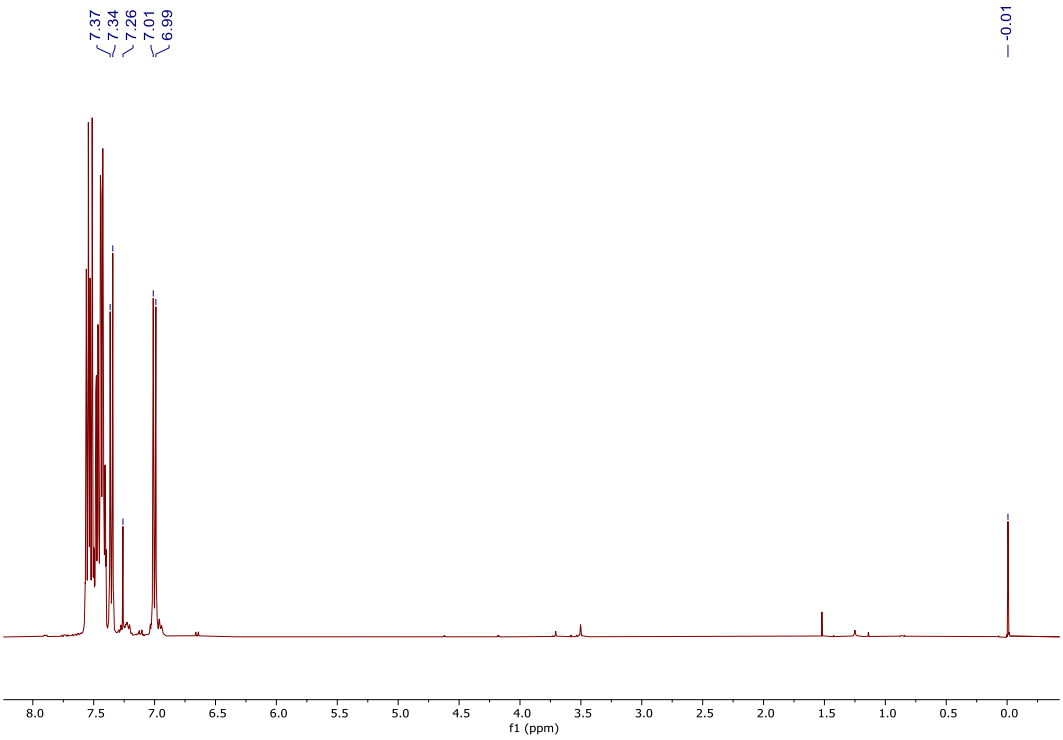

Figure S11. ^{1}H NMR spectrum of **4-AuPPh$_3$** ($CDCl_3$, 400 MHz).

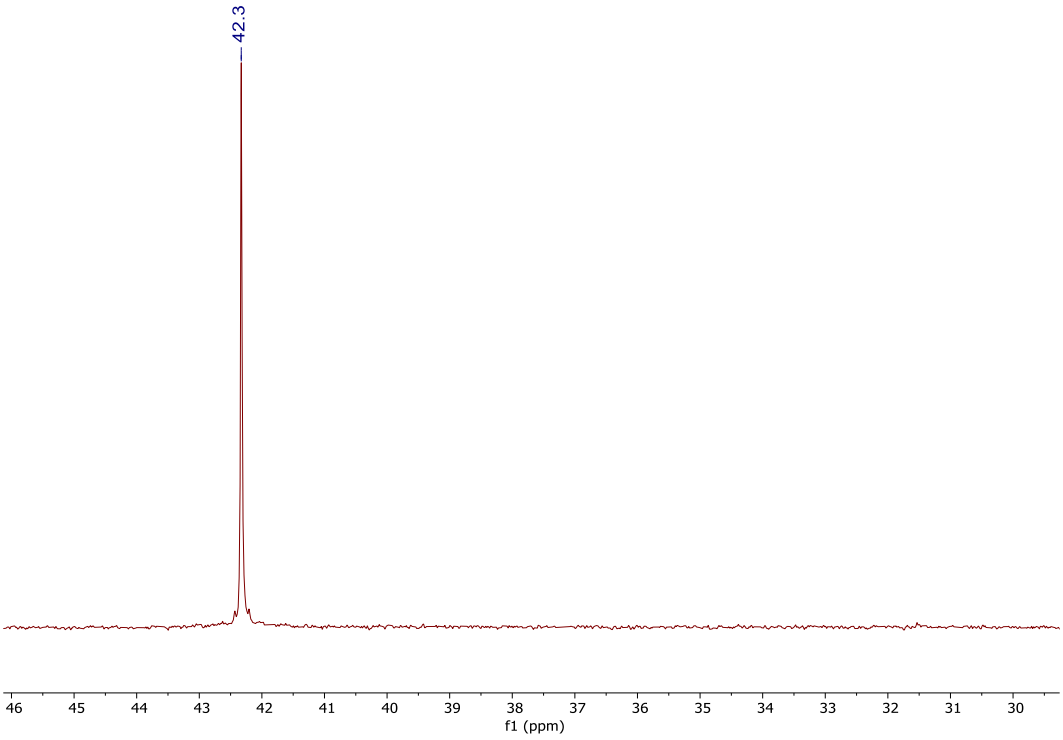

Figure S12. $^{31}P\{^{1}H\}$ NMR spectrum of **4-AuPPh$_3$** ($CDCl_3$, 162 MHz).

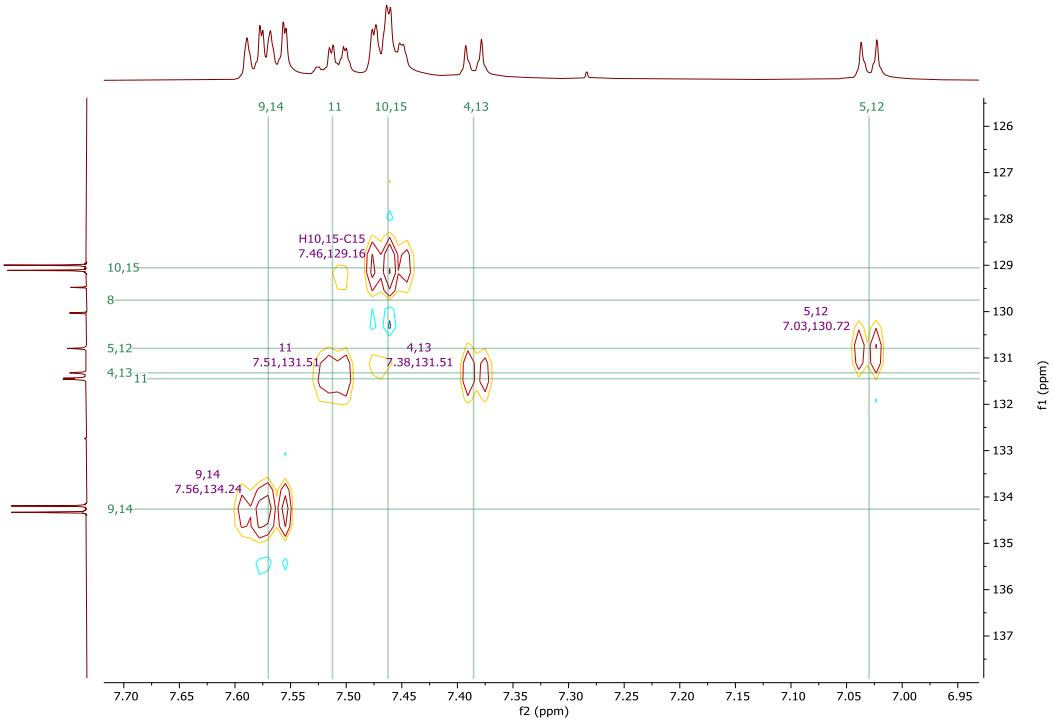

Figure S13. ^{1}H-^{13}C gHSQC spectrum of **4-AuPPh$_3$** ($CDCl_3$, 400 MHz).

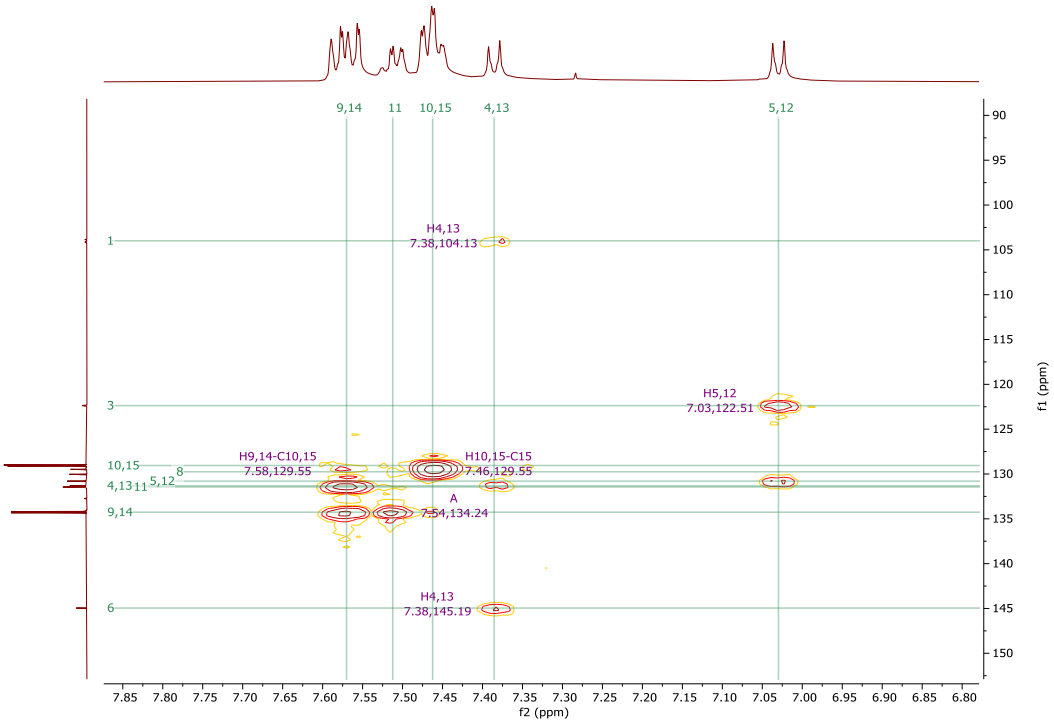

Figure S14. ^{1}H-^{13}C gHMBC spectrum of **4-AuPPh$_3$** ($CDCl_3$, 400 MHz).

1.6 X-Ray Crystallography of **4-AuPPh$_3$**

X-Ray Intensity data were collected at 100 K on a Bruker Dual micro source D8 Venture diffractometer and PHOTON III detector running APEX3 software package of programs and using Mo Kα radiation (λ = 0.71073 Å). The data frames were integrated, and multi-scan scaling was applied in APEX3. Intrinsic phasing structure solution provided all of the non-H atoms. The structure was refined using full-matrix least-squares refinement.[6] The non-H atoms were refined with anisotropic displacement parameters and all of the H atoms were calculated in idealized positions and refined riding on their parent atoms. The asymmetric unit consists of the Au_4 complex and seven dichloromethane solvent molecules. The dichloromethane molecules were disordered and could not be modeled properly, thus program SQUEEZE, a part of the PLATON[7] package of crystallographic software, was used to calculate the solvent disorder area and remove its contribution to the overall intensity data. The complex exhibits significant disorder in six of the twelve phenyl rings. Each phenyl ring disorder was refined in two parts with their site occupation factors adding to one. These disorders and the solvent disorder contribute significantly to the overall R-values. The SQEEZE parameters are as follows: Total potential solvent accessible void is 3189A3, and the electron count voids/cell is 1181 electrons. In the final cycle of refinement, 22883 reflections (of which 13770 are observed with $I > 2\sigma(I)$) were used to refine 668 parameters and the resulting R_1, wR_2 and S (goodness of fit) were 9.79%, 24.72% and 1.476, respectively. The refinement was carried out by minimizing the wR_2 function using F^2 rather than F values. R_1 is calculated to provide a reference to the conventional R value but its function is not minimized.

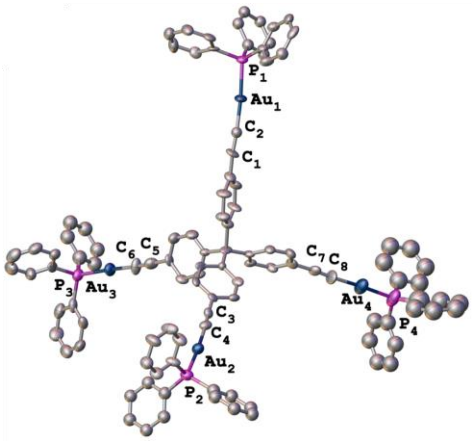

Figure S15. Molecular structure of **4-AuPPh$_3$** (Hydrogen atoms removed for clarity).

Table S2. Crystal data and structure refinement for **4-AuPPh$_3$**.

CCDC Number	**2158226**
Empirical formula	$C_{105}H_{76}Au_4P_4$
Formula weight	2451.24
Temperature	100(2) K
Wavelength	0.71073 Å
Crystal system	Monoclinic
Space group	$P2_1/n$
Unit cell dimensions	a = 17.554(2) Å, α= 90°. b = 33.635(5) Å, β= 94.532(2)°. c = 18.811(3) Å, γ= 90°.
Volume	11072(3) Å^3
Z	4
Density (calculated)	1.471 Mg/m^3
Absorption coefficient	5.480 mm^{-1}
F(000)	4720
Crystal size	0.469 x 0.317 x 0.174 mm^3
Theta range for data collection	1.949 to 26.547°.
Index ranges	-21≤h≤21, -42≤k≤41, -23≤l≤11
Reflections collected	70789
Independent reflections	22883 [R(int) = 0.0886]
Completeness to theta = 25.242°	99.9 %
Absorption correction	multi-scan
Refinement method	Full-matrix least-squares on F^2
Data / restraints / parameters	22883 / 4 / 668
Goodness-of-fit on F^2	1.476
Final R indices [I>2sigma(I)]	R_1 = 0.0979, wR_2 = 0.2472 [13770]
R indices (all data)	R_1 = 0.1588, wR_2 = 0.2689
Extinction coefficient	n/a
Largest diff. peak and hole	4.541 and -1.921 e.Å^{-3}

1.7 Synthesis of **7-AuPPh$_3$**

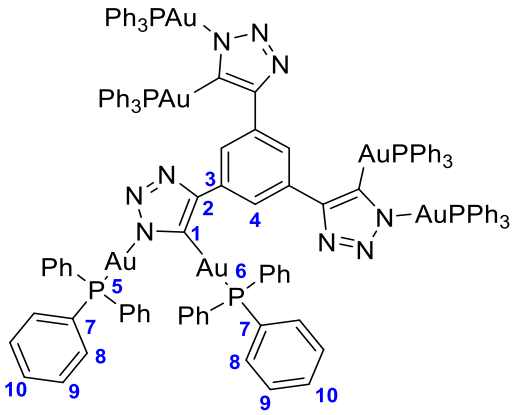

1-AuN$_3$ (25.0 mg, 0.0500 mmol) and **3-AuPPh$_3$** (25.4 mg, 0.0167 mmol) were dissolved in 1.5 mL of $CDCl_3$. The reaction mixture was transferred into a sealable NMR tube and monitored with ^1H and ^{31}P NMR spectroscopy. The reaction was stopped at 12 h. The mixture was filtered and the solid was washed 3x with 5 mL CH_2Cl_2 to yield a yellow powder. 92% Yield (46.4 mg). ^1H NMR (400 MHz, $CDCl_3$): δ 9.00 (s), 8.45 (m), 7.67-6.90 (m). $^{13}C\{^1H\}$ NMR (101 MHz, $CDCl_3$)): δ 151.8 (s, C_2), 134.1 (s, C_8), 131.7 (s, C_{10}), 131.1 (s, C_7), 129.2 (s, C_9), 124.7 (s, C_4). $^{31}P\{^1H\}$ NMR (162 MHz, $CDCl_3$): δ 43.7 (s, P_6), 30.6 (s, P_5).

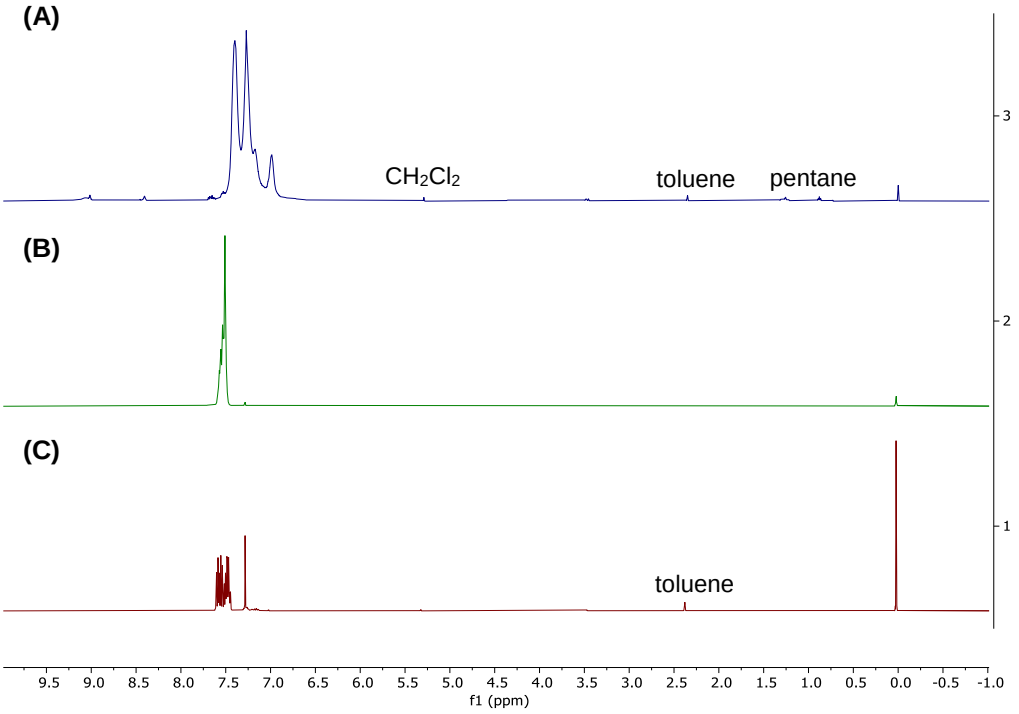

Figure S16. ^{1}H NMR spectrum of (A) **7-AuPPh$_3$**, (B) **1-AuN$_3$**, (C) **3-AuPPh$_3$** ($CDCl_3$, 400 MHz).

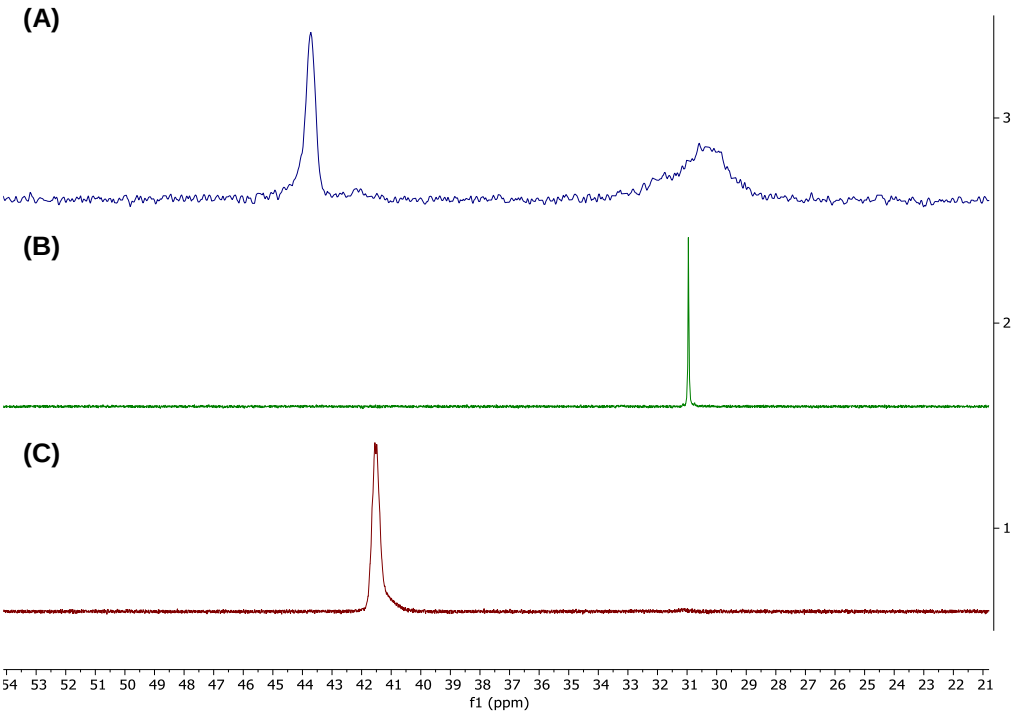

Figure S17. ^{31}P{^{1}H} spectrum of (A) **7-AuPPh$_3$**, (B) **1-AuN$_3$**, (C) **3-AuPPh$_3$** ($CDCl_3$, 162 MHz).

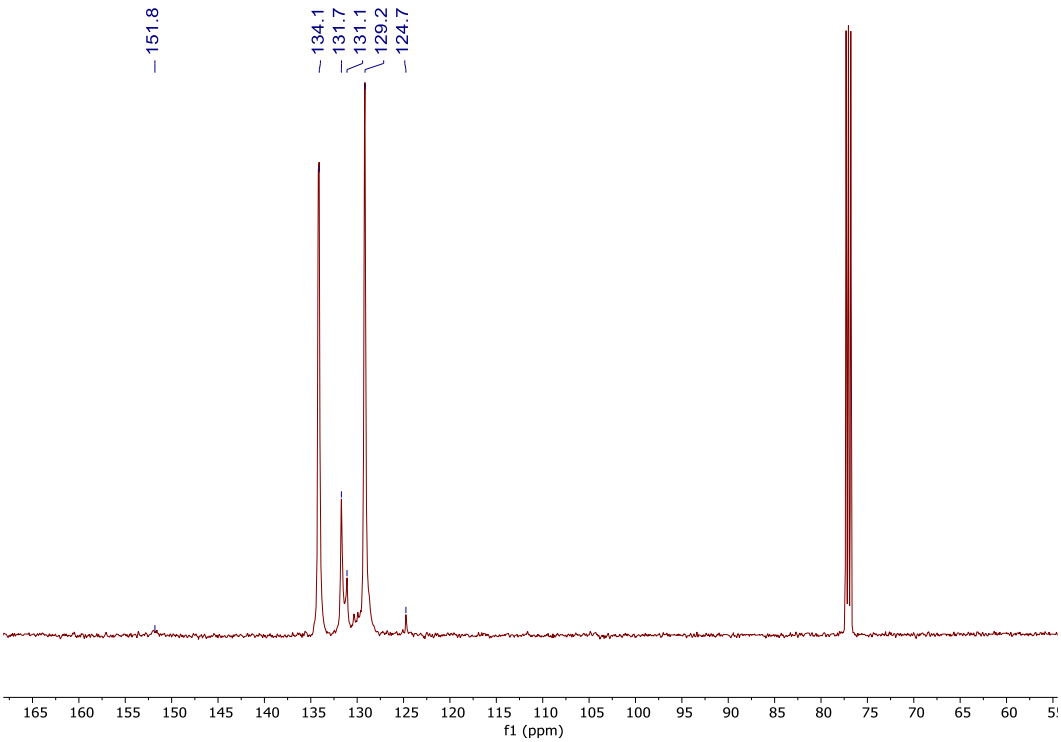

Figure S18. $^{13}C\{^{1}H\}$ NMR spectrum of **7-AuPPh$_3$** ($CDCl_3$, 101 MHz).

1.9 Synthesis of **7-AuPEt$_3$**

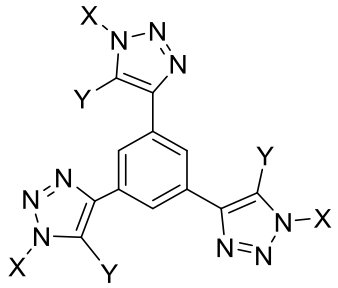

X = AuPPh$_3$, Y = AuPEt$_3$;
X = AuPPh$_3$, Y = AuPPh$_3$;
X = AuPEt$_3$, Y = AuPEt$_3$;
X = AuPEt$_3$, Y = AuPPh$_3$.

The same synthesis and workup procedure to that described previously for **7-AuPPh$_3$** was followed, using **1-AuN$_3$** (25.0 mg, 0.0500 mmol) and **3-AuPEt$_3$** (18.2 mg, 0.0167 mmol) to yield a yellow powder. 85% Yield (0.0141 mmol, 36.6 mg). ^{1}H NMR (600 MHz, $CDCl_3$): δ 7.82 (m), 7.70-7.65 (m), 7.57-7.44 (m), 1.84 (m, Et), 1.20 (m, Et). $^{13}C\{^1H\}$ NMR (151 MHz, $CDCl_3$)): δ 134.2 (d, *J* = 6 Hz), 133.4 (d, *J* = 12 Hz), 133.1 (d, *J* = 3 Hz), 132.5 (d, *J* = 5 Hz), 132.1 (d, *J* = 4 Hz), 132.0 (s), 129.2 (d, *J* = 4 Hz), 128.5 (d, *J* = 5 Hz), 126.5 (d, *J* = 48 Hz), 17.9 (d, *J* = 16 Hz, Et), 9.05 (s, Et). $^{31}P\{^1H\}$ NMR (243 MHz, $CDCl_3$): δ 52.6 (s), 42.2 (s), 37.7 (s), 33.2 (s), 31.6 (s), 31.0 (s), 29.2 (s), 24.5 (s).

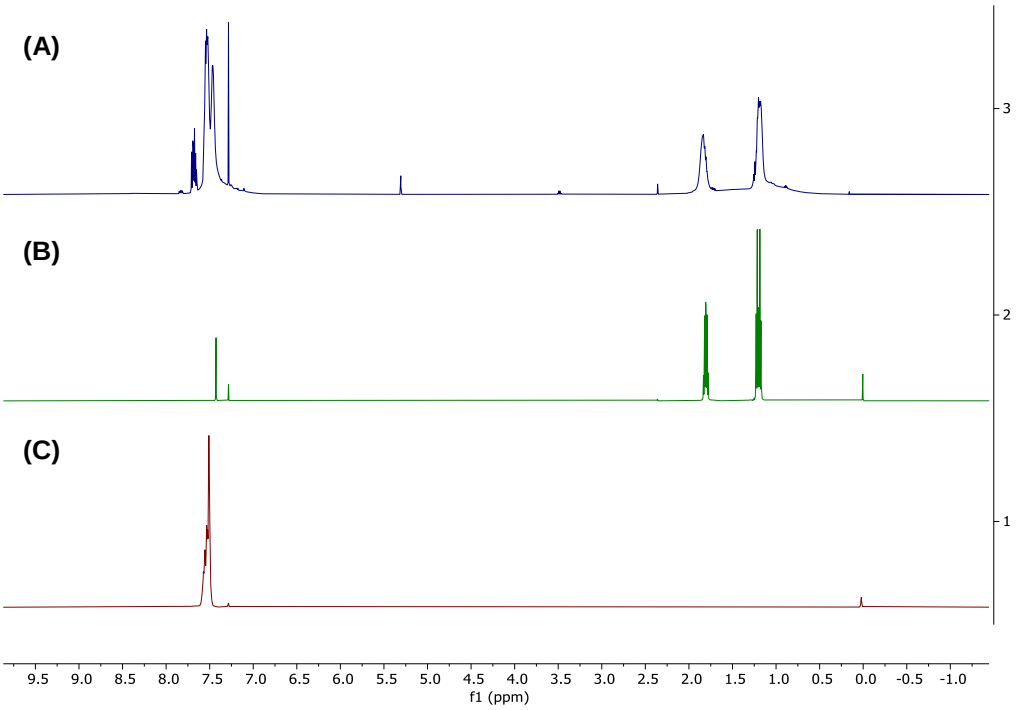

Figure S19. ^{1}H NMR spectrum of (A) **7-AuPEt$_3$**, (B) **3-AuPEt$_3$**, (C) **1-AuN$_3$** ($CDCl_3$, 600 MHz).

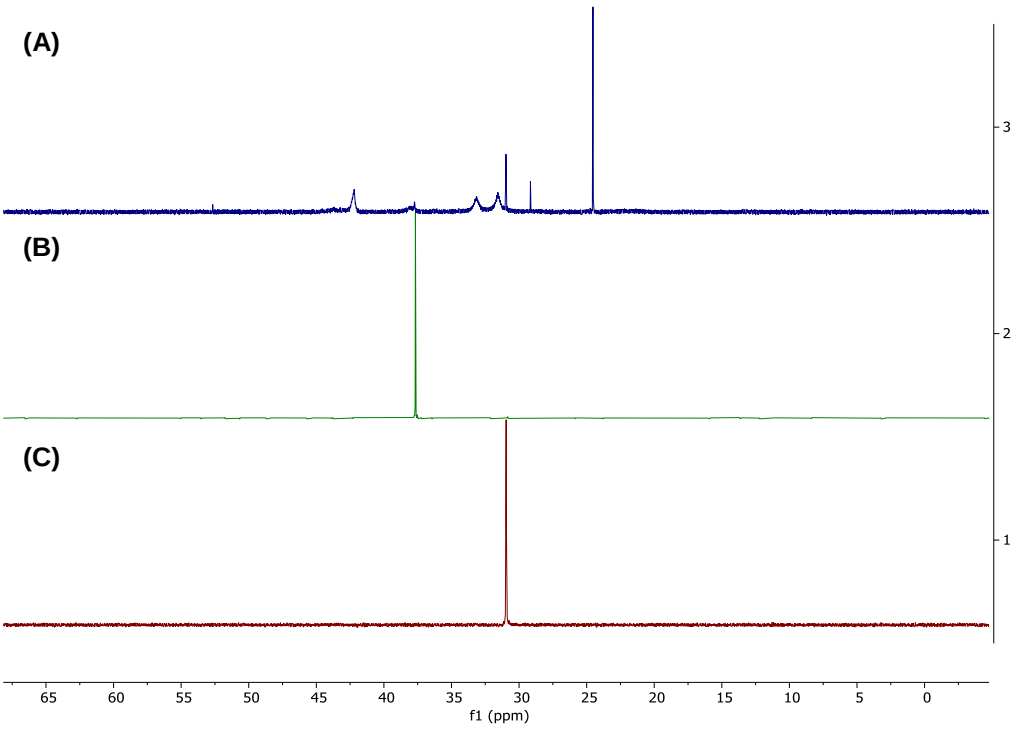

Figure S20. ^{31}P{^{1}H} spectrum of (A) **7-AuPEt$_3$**, (B) **3-AuPEt$_3$**, (C) **1-AuN$_3$** ($CDCl_3$, 243 MHz).

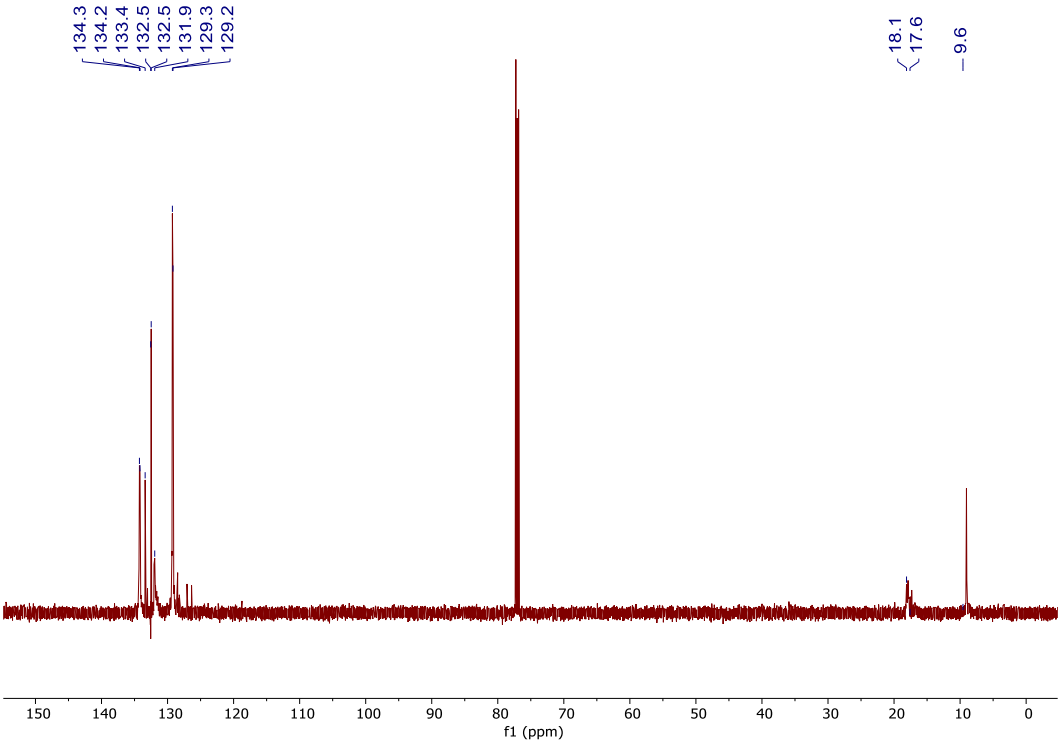

Figure S21. $^{13}C\{^{1}H\}$ NMR spectrum of **7-AuPEt$_3$** ($CDCl_3$, 151 MHz).

1.8 Synthesis of **8-AuPPh$_3$**

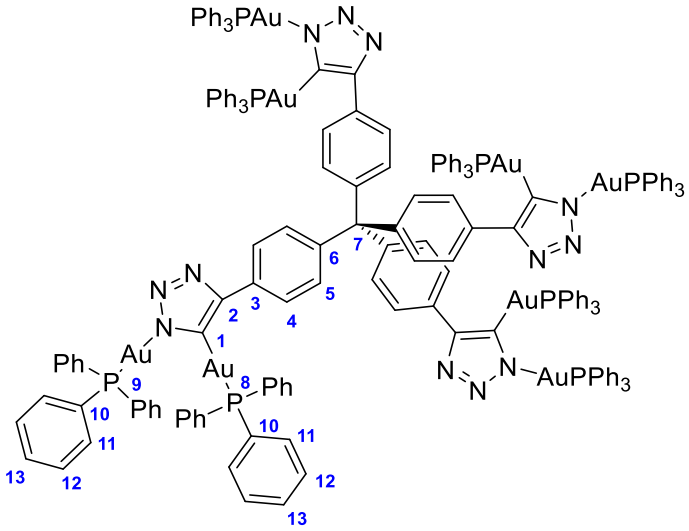

The same synthesis and workup procedure to that described previously for **7-AuPPh$_3$** was followed, using **1-AuN$_3$** (25.0 mg, 0.0500 mmol) and **4-AuPPh$_3$** (28.0 mg, 0.0125 mmol) to yield a yellow powder. 95% Yield (50.3 mg). ^{1}H NMR (400 MHz, $CDCl_3$): δ 8.40 (d, $^{3}J_{HH}$ = 8.29 Hz, C_4-H), 7.59-6.88 (m). $^{13}C\{^{1}H\}$ NMR (101 MHz, $CDCl_3$)): δ 151.5 (s, C_1), 145.2 (s, C_2), 134.0 (d, $^{2}J_{CP}$ = 4.8 Hz, C_{11}), 131.7 (s, C_{13}), 129.1 (d, $^{3}J_{CP}$ = 1.2 Hz, C_{12}), 125.8 (s, C_{10}), 64.2 (C_7). $^{31}P\{^{1}H\}$ NMR (162 MHz, $CDCl_3$): δ 44.2 (s, P_8), 30.8 (s, P_9).

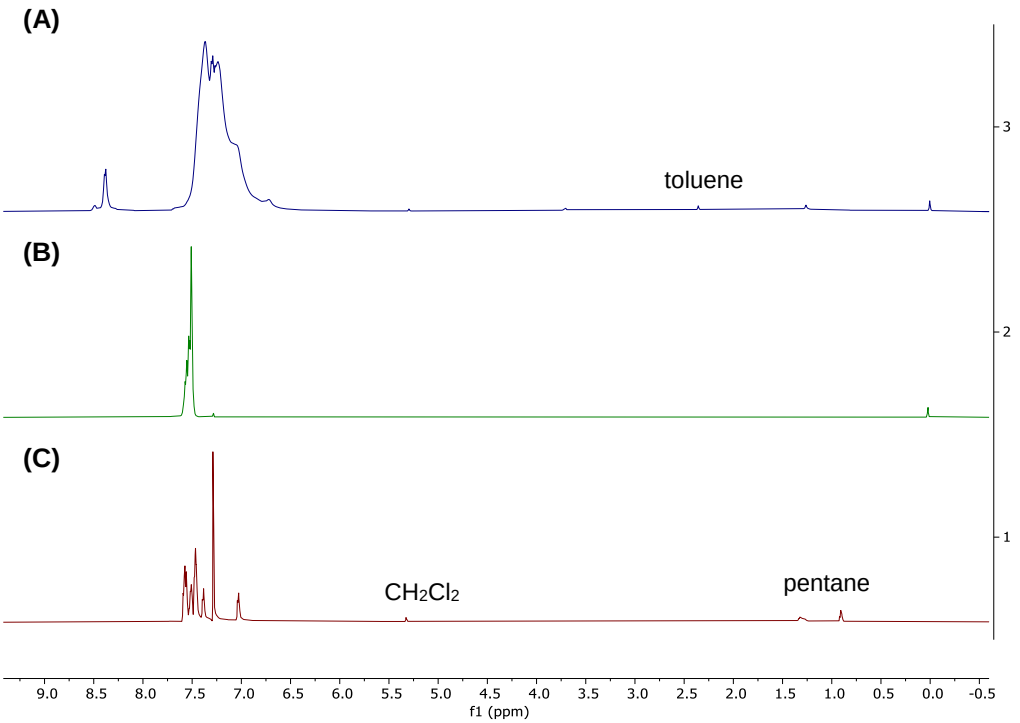

Figure S22. ^{1}H NMR spectrum of (A) **8-AuPPh$_3$**, (B) **1-AuN$_3$**, (C) **4-AuPPh$_3$** ($CDCl_3$, 400 MHz).

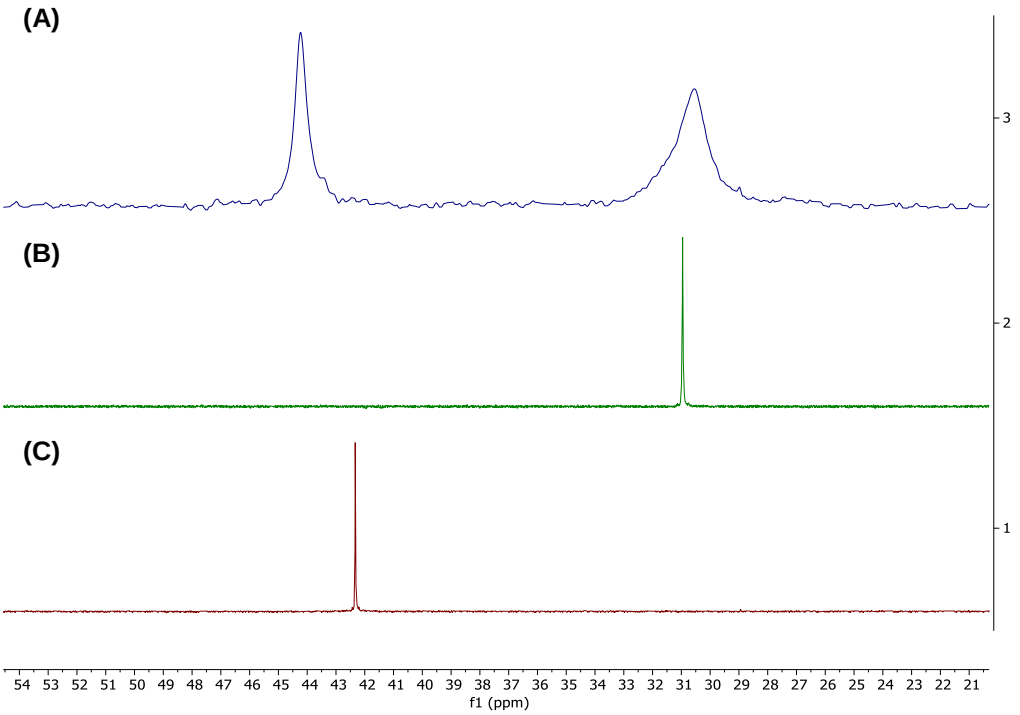

Figure S23. ^{31}P{^{1}H} spectrum of (A) **8-AuPPh$_3$**, (B) **1-AuN$_3$**, (C) **4-AuPPh$_3$** ($CDCl_3$, 162 MHz).

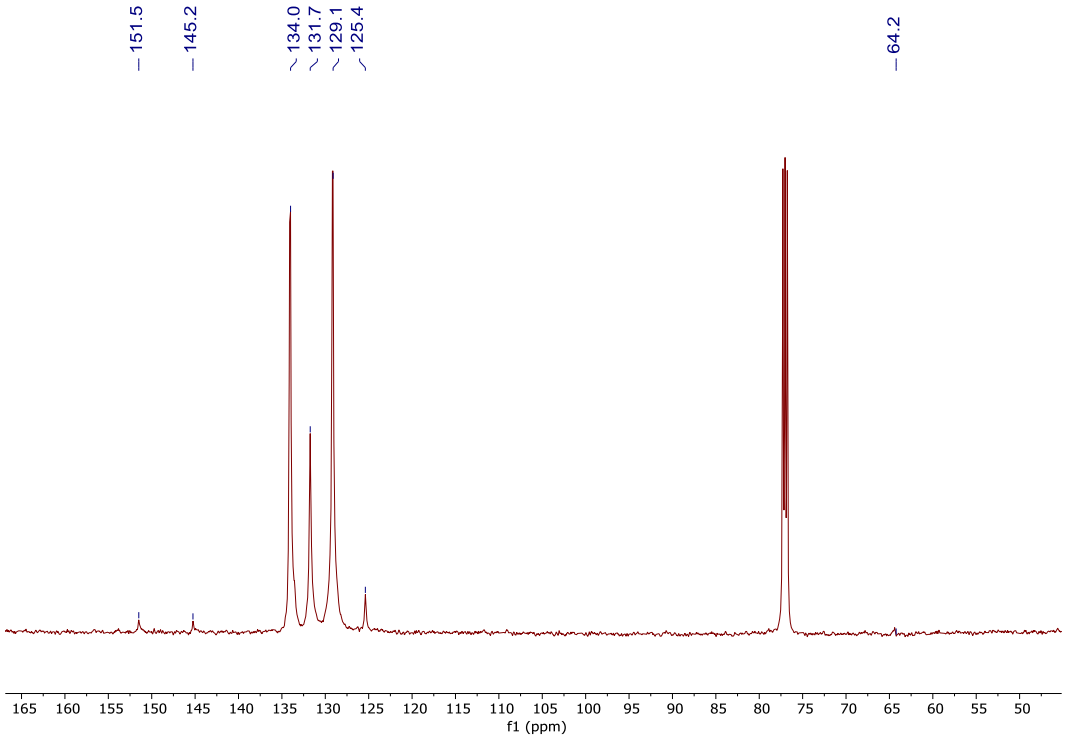

Figure S24. $^{13}C\{^{1}H\}$ NMR spectrum of **8-AuPPh$_3$** ($CDCl_3$, 101 MHz).

1.9 Synthesis of **7-H**

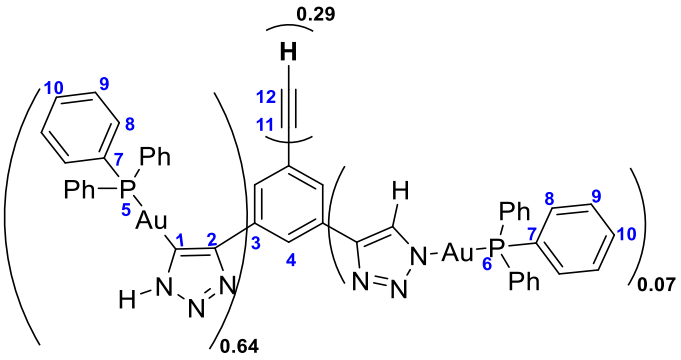

The same synthesis and workup procedure to that described previously for **7-AuPPh$_3$** was followed, using **1-AuN$_3$** (25.0 mg, 0.0500 mmol) and **3-H** (2.5 mg, 0.017 mmol) to yield a yellow powder. 82% Yield (22.6 mg). ^{1}H NMR (400 MHz, $CDCl_3$): δ 11.85 (s, N-H), 9.23 (s, C_4-H), 9.11 (s, C_4-H), 8.35 (s, C_4-H), 7.47-7.37 (m, C_8-H, C_9-H, C_{10}-H), 3.47 (s, C_{12}-H), 3.32 (s, C_{12}-H), 2.91 (s, C_{12}-H). ^{13}C{^{1}H} NMR (101 MHz, $CDCl_3$)): δ 135.2 (s, C_3), 134.2 (d, $^{2}J_{CP}$ = 8 Hz, C_8), 131.5 (s, C_{10}), 129.8 (m, C_7), 129.3 (d, $^{3}J_{CP}$ = 4 Hz, C_9), 124.4 (s, C_4). ^{31}P{^{1}H} NMR (162 MHz, $CDCl_3$): δ 43.3 (s, P_5), 29.9 (s, P_6).

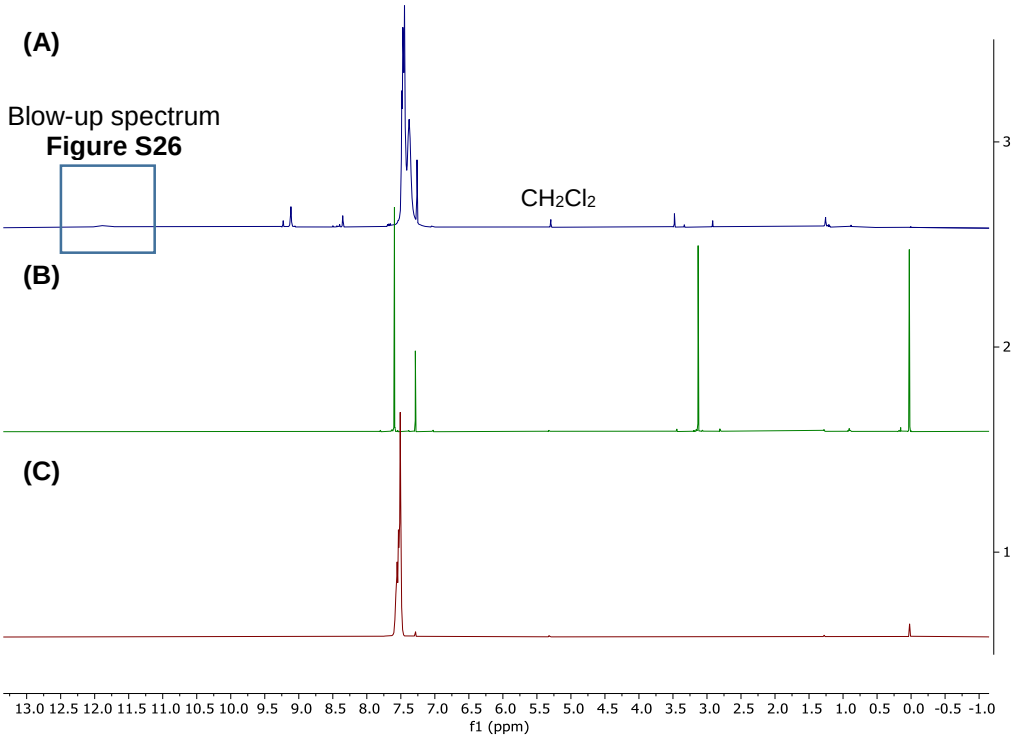

Figure S25. ^{1}H NMR spectrum of (A) **7-H**, (B) **3-H**, (C) **1-AuN$_3$** ($CDCl_3$, 400 MHz).

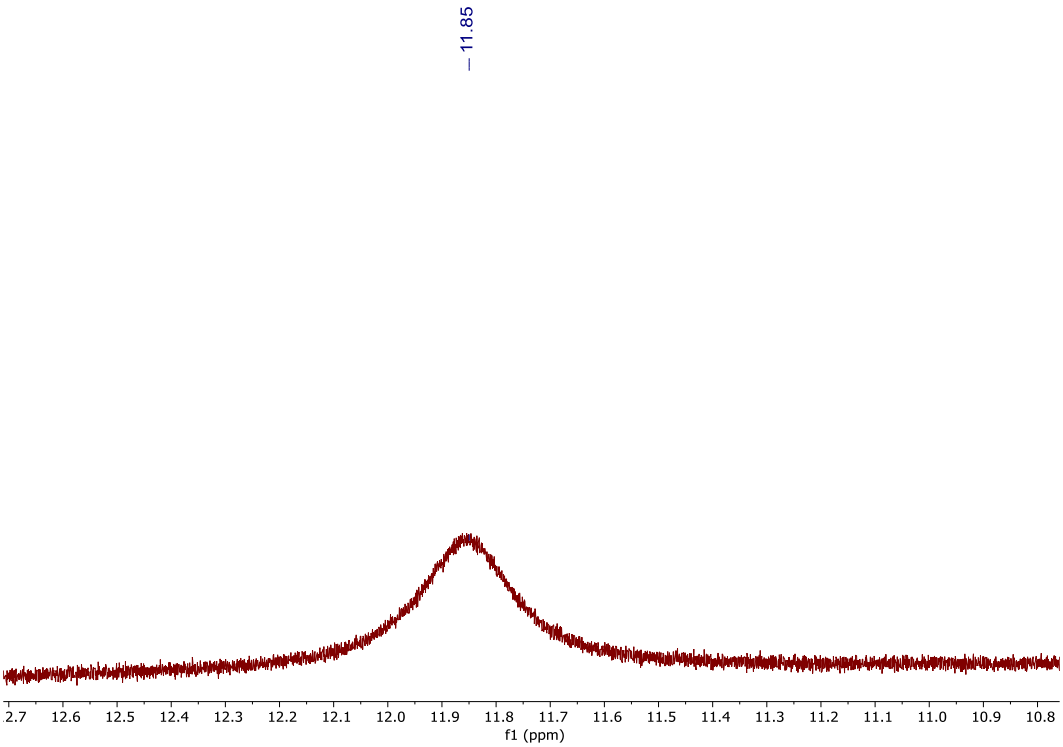

Figure S26. Blow-up ^{1}H spectrum of **7-H** from 10.8-12.7 ppm ($CDCl_3$, 400 MHz).

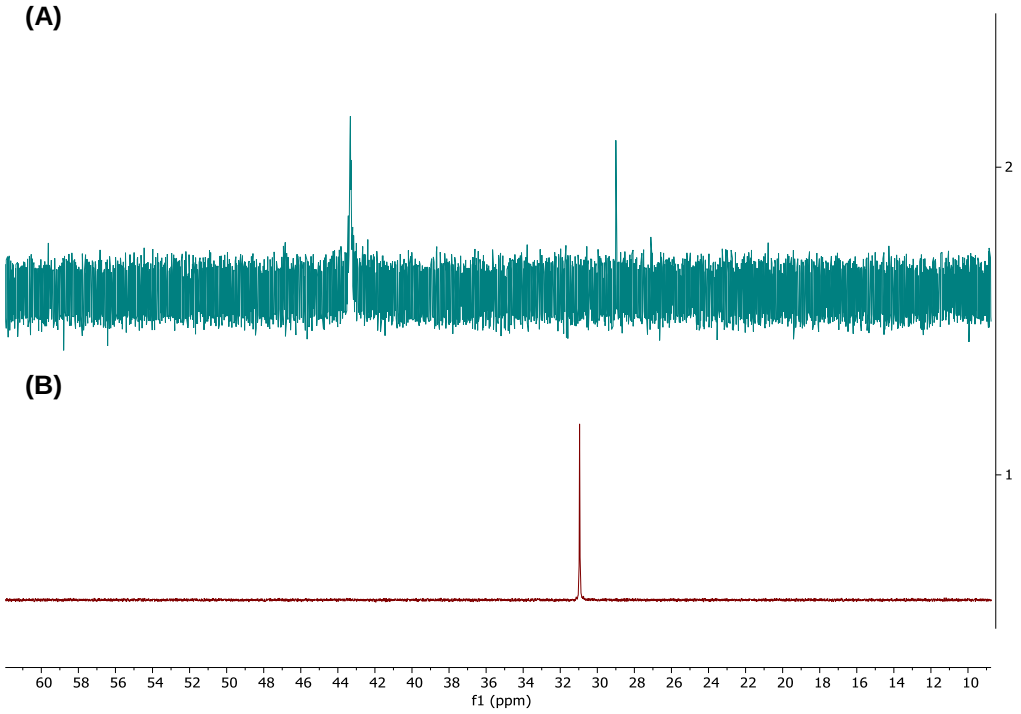

Figure S27. $^{31}P\{^{1}H\}$ spectrum of (A) **7-H** and (B) **1-AuN$_3$** ($CDCl_3$, 162 MHz).

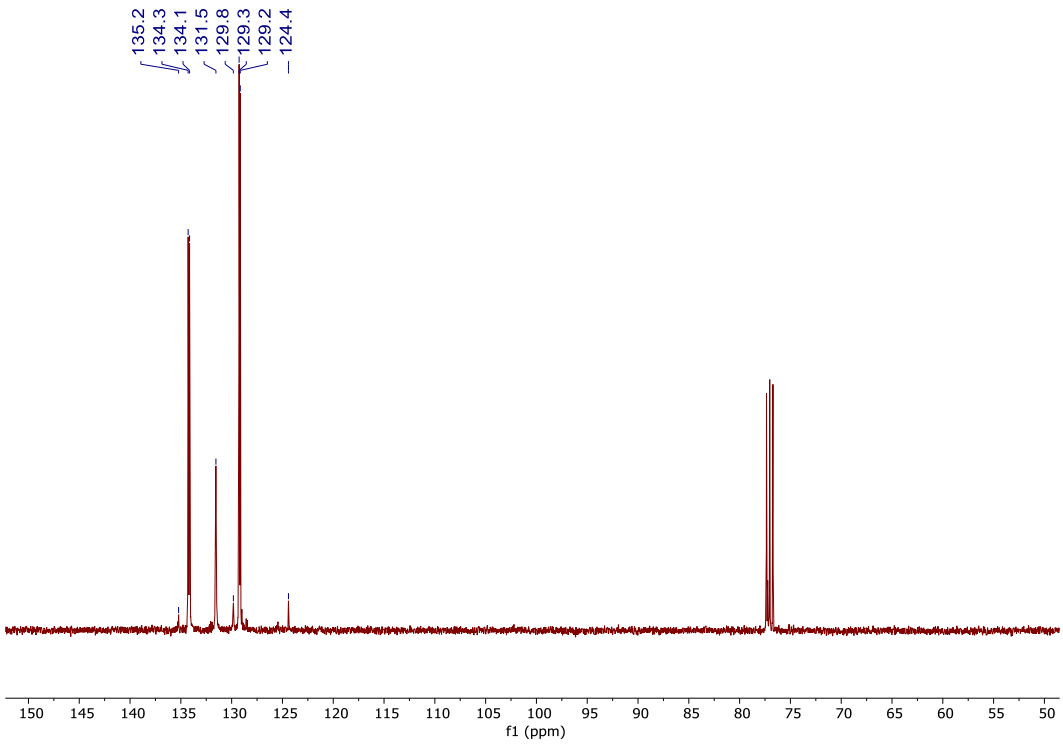

Figure S28. $^{13}C\{^{1}H\}$ NMR spectrum of **7-H** ($CDCl_3$, 101 MHz).

1.10 Synthesis of **8-H**

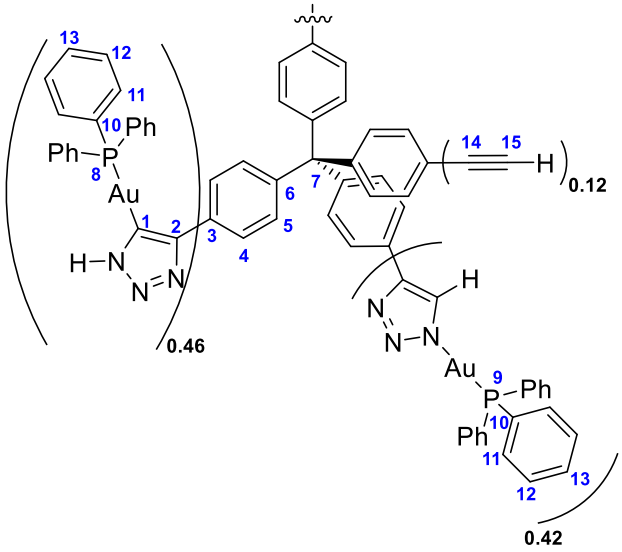

The same synthesis and workup procedure to that described previously for **7-AuPPh$_3$** was followed, using **1-AuN$_3$** (25.0 mg, 0.0500 mmol) and **4-H** (5.2 mg, 0.0123 mmol) to yield a yellow powder. 91% Yield (27.5 mg). ^{1}H NMR (400 MHz, $CDCl_3$): δ 11.66 (s, N-H), 8.29-8.20 (m, C_4-H), 7.59 (m), 7.46-7.05 (m), 3.67 (m, C_{15}-H), 3.40 (q, J = 8 Hz, C_{15}-H), 3.00 (s, C_{15}-H). ^{13}C{^{1}H} NMR (101 MHz, $CDCl_3$)): δ 134.0 (d, $^2J_{CP}$ = 20 Hz, C_{11}), 131.9 (s, C_5), 131.4 (s, C_{13}), 129.3 (d, $^3J_{CP}$ = 4 Hz, C_{12}), 125.7 (s, C_4). ^{31}P{^{1}H} NMR (162 MHz, $CDCl_3$): δ 43.3 (s, P_8), 29.0 (s, P_9).

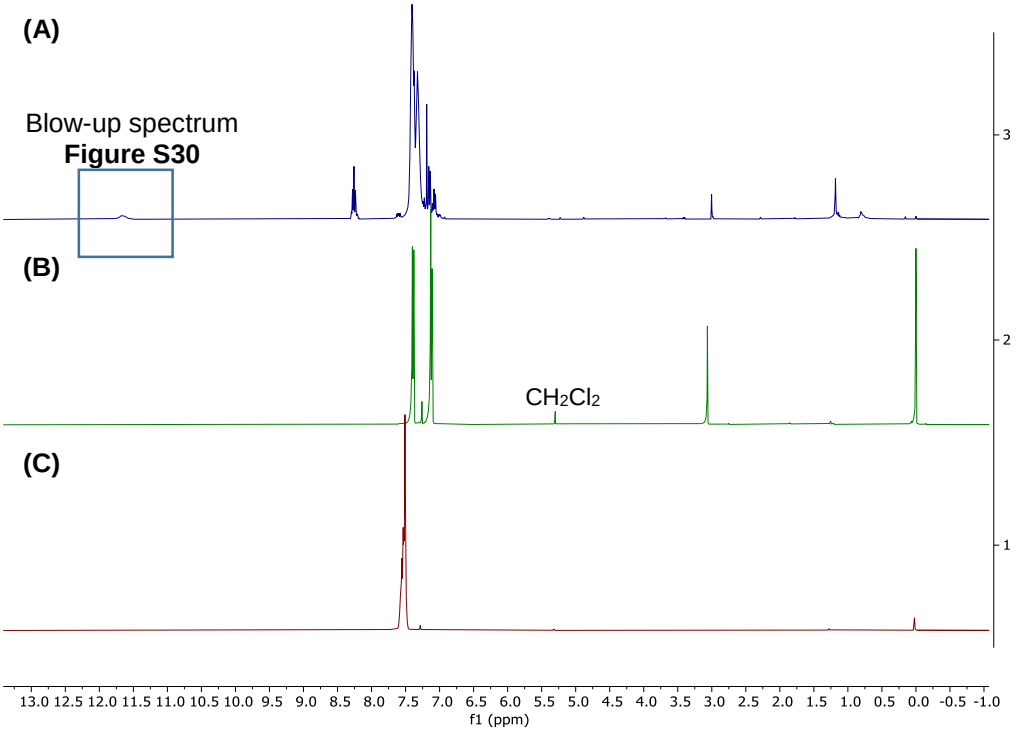

Figure S29. ^{1}H NMR spectrum of (A) **8-H**, (B) **4-H**, (C) **1-AuN$_3$** ($CDCl_3$, 400 MHz).

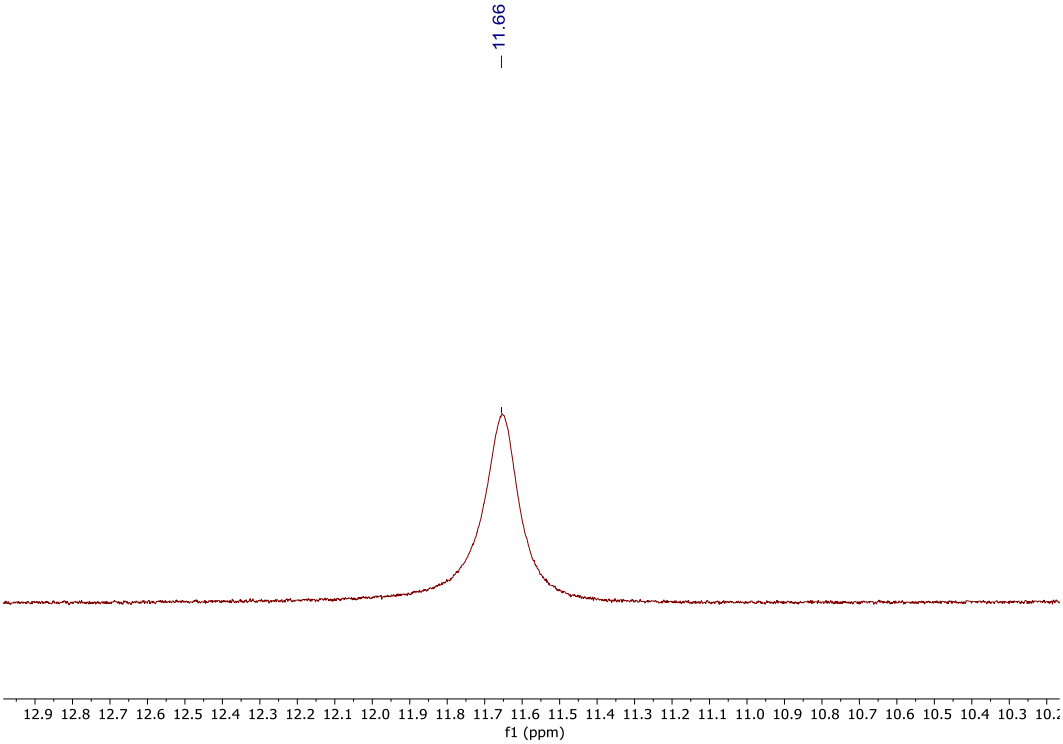

Figure S30. Blow-up ^{1}H spectrum of **8-H** from 10.3-12.9 ppm ($CDCl_3$, 400 MHz).

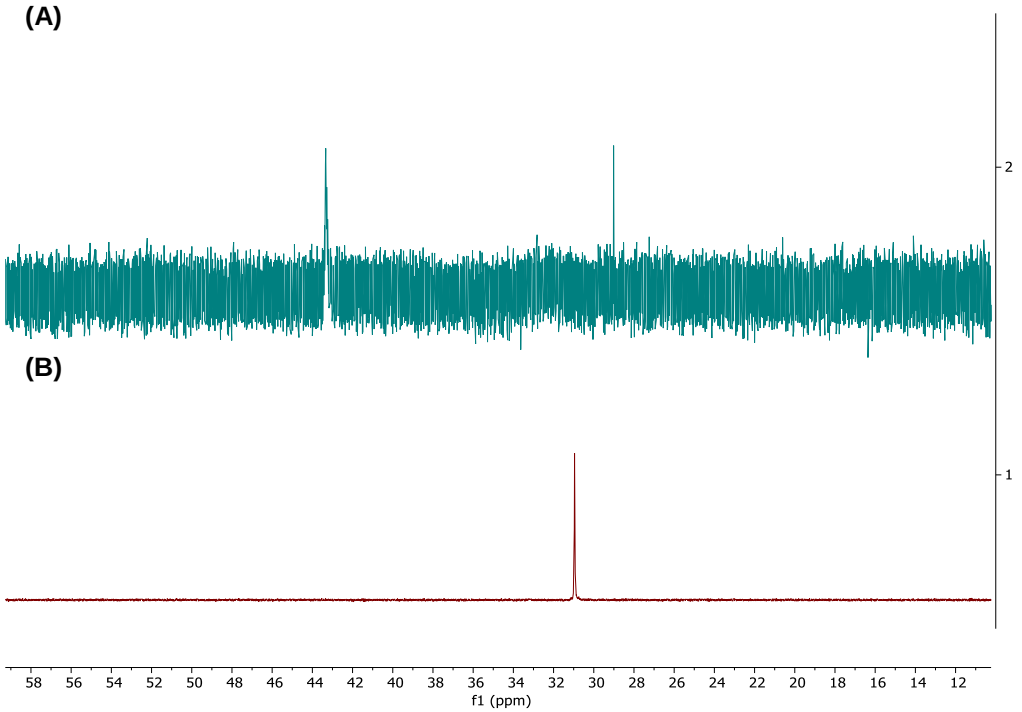

Figure S31. $^{31}P\{^{1}H\}$ spectrum of (A) **8-H** and (B) **1-AuN$_3$** ($CDCl_3$, 162 MHz).

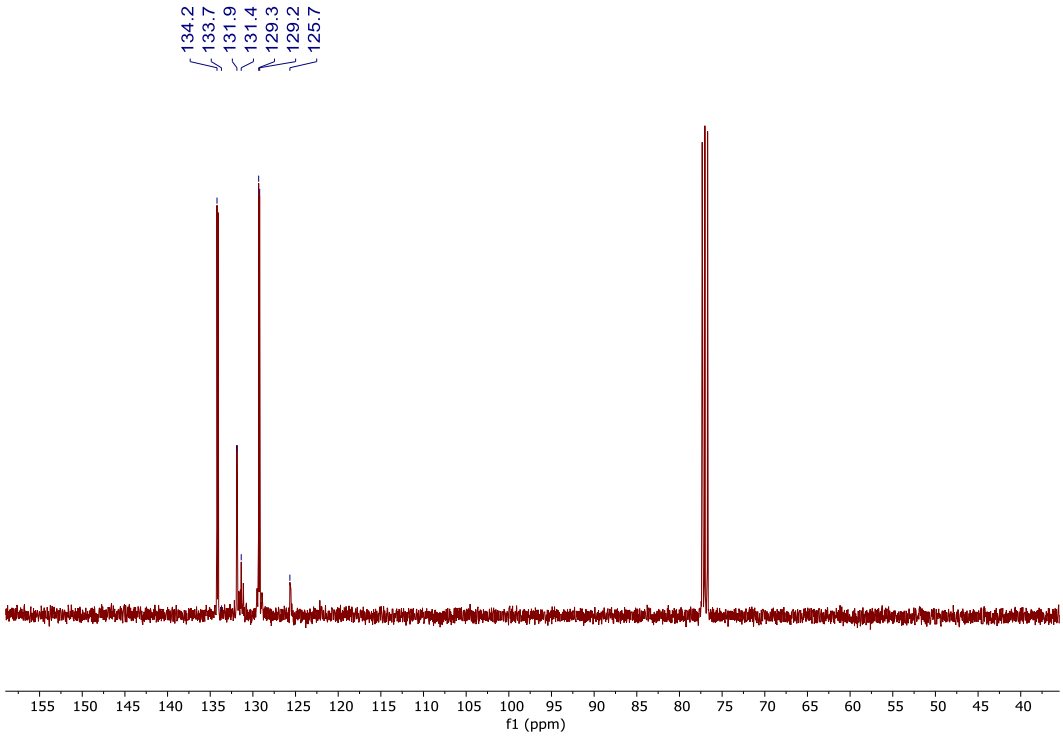

Figure S32. $^{13}C\{^{1}H\}$ NMR spectrum of **8-H** ($CDCl_3$, 101 MHz).

1.11 FTIR Spectra of Model Complexes

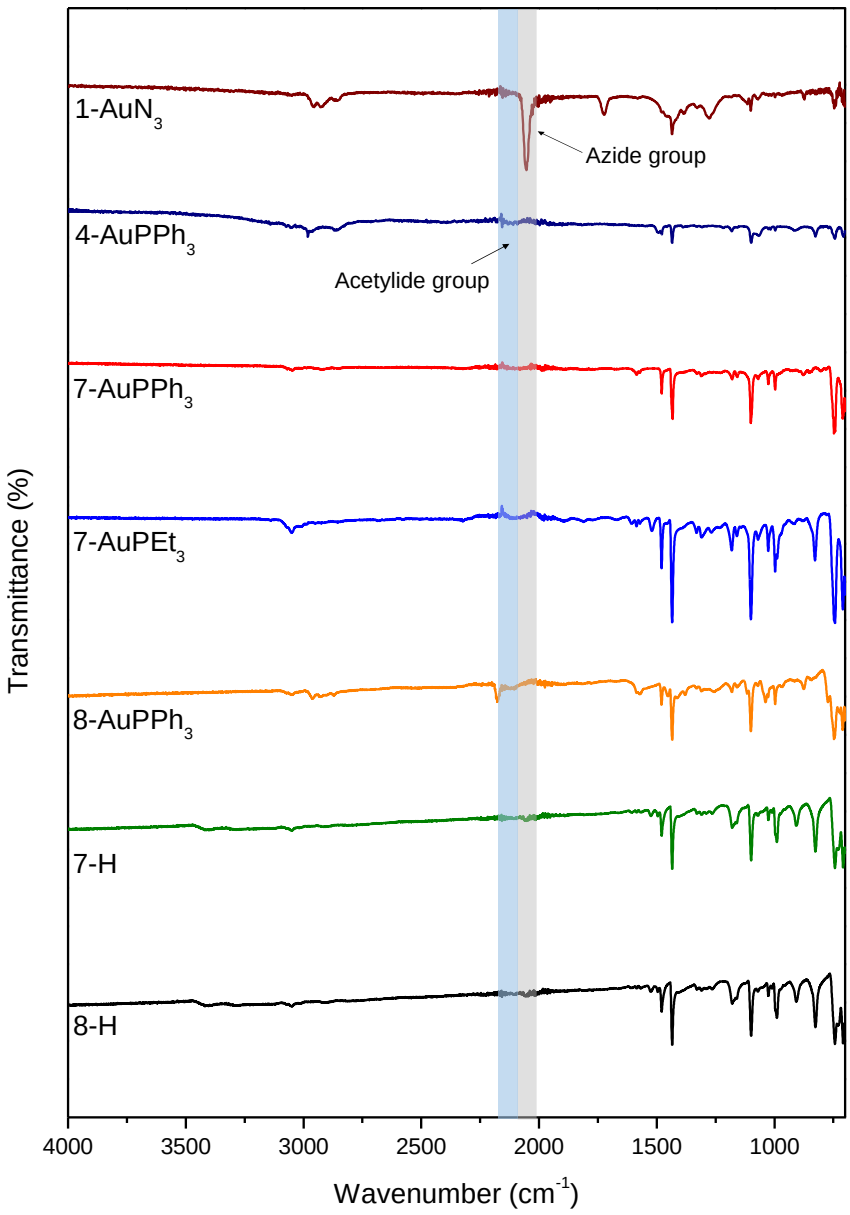

Figure S33. FTIR spectra of model complexes (**7-AuPPh$_3$**, **7-AuPEt$_3$**, **7-H**, **8-AuPPh$_3$**, and **8-H**) in comparison with **1Au-N$_3$** and **4-AuPPh$_3$**.

2. Syntheses and Isolation of iClick Network Metallopolymers

2.1 Synthesis of **5-AuPPh$_3$**, **5-AuPEt$_3$**, and **6-AuPPh$_3$**

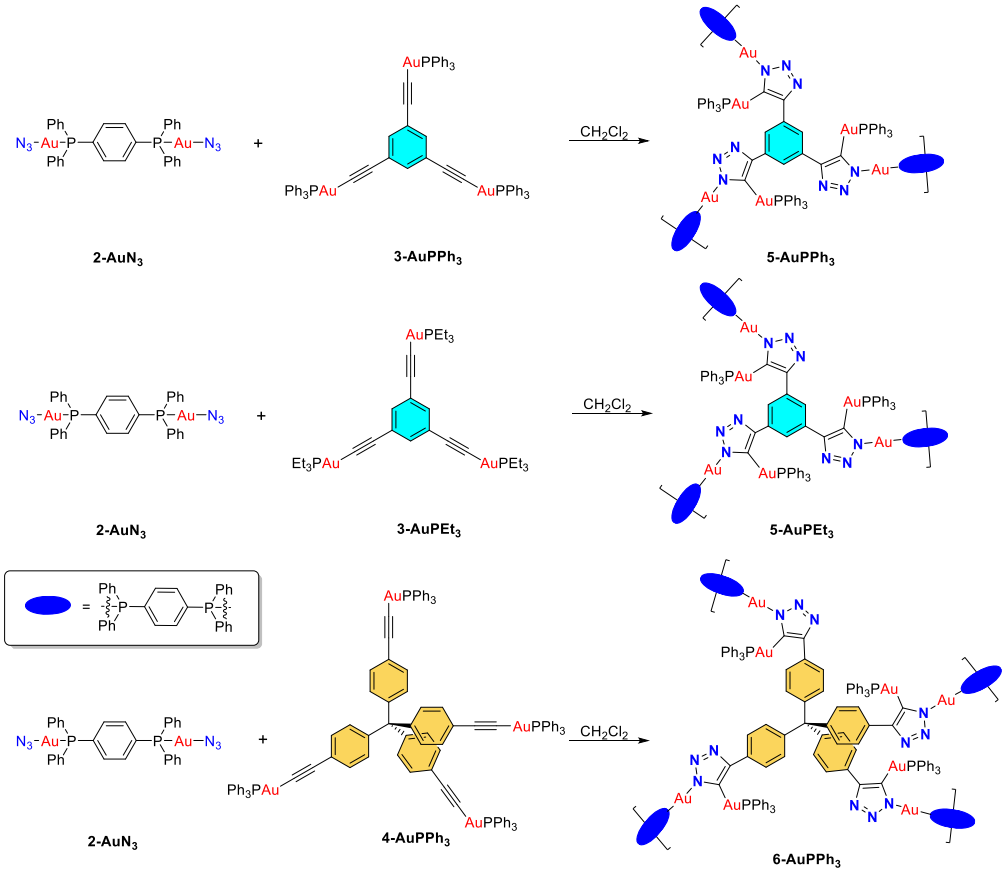

Scheme S1. The idealized structure of iClick network metallopolymers **5-AuPPh$_3$**, **5-AuPEt$_3$**, and **6-AuPPh$_3$**.

*Synthesis of **5-AuPEt$_3$*** (**Table S3**, entry **5-AuPEt$_3$**)

2-AuN$_3$ (160.0 mg, 0.1731 mmol) and **3-AuPEt$_3$** (126.5 mg, 0.1157 mmol) were weighed out in different vials and CH_2Cl_2 was added to both vials until all materials were fully dissolved (30 mL for **2-AuN$_3$**; 4 mL for **3-AuPEt$_3$**). The colorless **2-AuN$_3$** solution was first transferred into a pressure tube then the yellow **3-AuPEt$_3$** solution was slowly added while stirring rigorously. Upon mixing, the solution turned from a transparant yellow solution to an opaque cream color. The pressure tube was later heated at 50 °C for 6 d. During the heating process precipitates from and after 6 days pink solids form and a transparent colorless supernatant are observed.

The reaction was cooled to room temperature and the mixture was filtered over a coarse filter paper. The resulting pink solid was collected then stirred with 30 mL of CH_2Cl_2

at room temperature for 1 h before being filtered over a coarse filter paper. The solid was later washed with CH_2Cl_2 (20 mL, 3x). 95% Yield (270.9 mg).

Synthesis of ***5-AuPPh$_3$*** (**Table S3**, entry **5-AuPPh$_3$-2)**

The same synthesis and workup procedure to that described previously for **5-AuPEt$_3$** was followed, **3-AuPPh$_3$** (177.6 mg, 0.1165 mmol) in 6 mL CH_2Cl_2 was slowly added into **2-AuN$_3$** (161.5 mg, 0.1747 mmol) in 30 mL CH_2Cl_2 to yield a pink powder. 76% Yield (257.7 mg).

Synthesis of ***6-AuPPh$_3$*** (**Table S3**, entry **6-AuPPh$_3$-2)**

The same synthesis and workup procedure to that described previously for **5-AuPEt$_3$** was followed, using **2-AuN$_3$** (160.0 mg, 0.1731 mmol) in 30 mL CH_2Cl_2 and **4-AuPPh$_3$** (172.9 mg, 0.0864 mmol) in 8 mL CH_2Cl_2 to yield a pink powder. 82% Yield (221.4 mg).

2.2 Synthesis of **5-H** and **6-H**

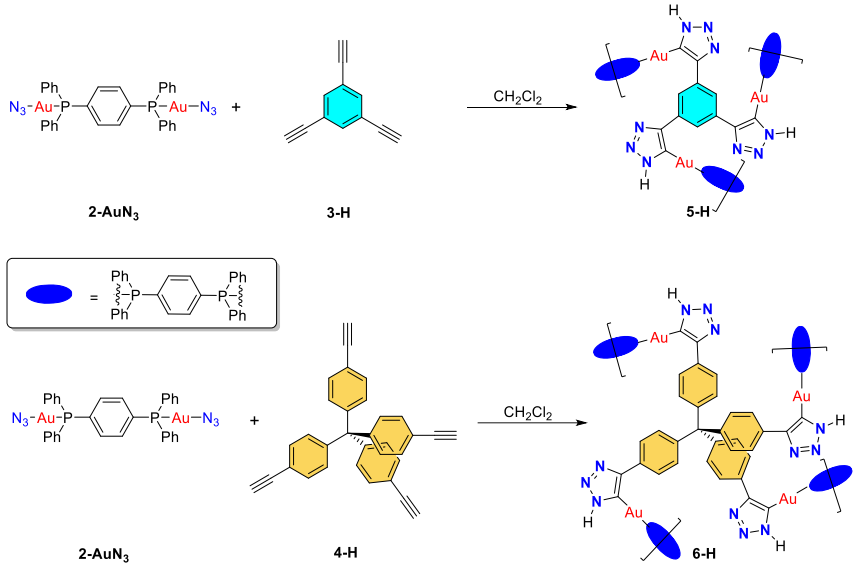

Scheme S2. The idealized structure of iClick network metallopolymers **5H** and **6H**.

*Synthesis of **5-H*** (**Table S3**, entry **5H-1)**

2-AuN$_3$ (236.3 mg, 0.2556 mmol) and **3-H** (25.6 mg, 0.170 mmol) were dissolved in CH_2Cl_2 (**2-AuN$_3$**: 40 ml; **3-H**: 2 ml) separately in different vials then slowly mixed together in a pressure tube. The slightly yellow transparant solution mixture was heated at 50 °C for 1 d before workup. A color change was observed after heating for 1 h; the solution turned to a milky light yellow color. After 1 d, the solution remained the same color and no solid precipitates were observed.

The reaction mixture was cooled to room temperature and the solvent was removed in vacuo. A white powder was collected and stirred with 20 mL of CH_2Cl_2 for 1 h at room temperature before being filtered over a coarse filter paper. The solid was later washed with CH_2Cl_2 (20 mL, 3x). 83% Yield (216.5 mg).

*Synthesis of **6-H*** (**Table S3**, entry **6-H)**

The same procedure of the synthesis of **5-H** was used for **6-H**. **2-AuN$_3$** (206.5 mg, 0.2234 mmol), **4-H** (46.5 mg, 0.112 mmol) were dissolved in CH_2Cl_2 (**2-AuN$_3$**: 40 ml; **4-H**: 6 ml) in separate vials and slowly mixed together in the pressure tube. The tube was heated at 50 °C for 1 d to form a white milky solution. The isolation process was same as describe for complex **5-H**. 86% Yield (217.4 mg).

3. Characterization of iClick Network Metallopolymers

3.1 FTIR spectra of iClick Network Metallopolymers

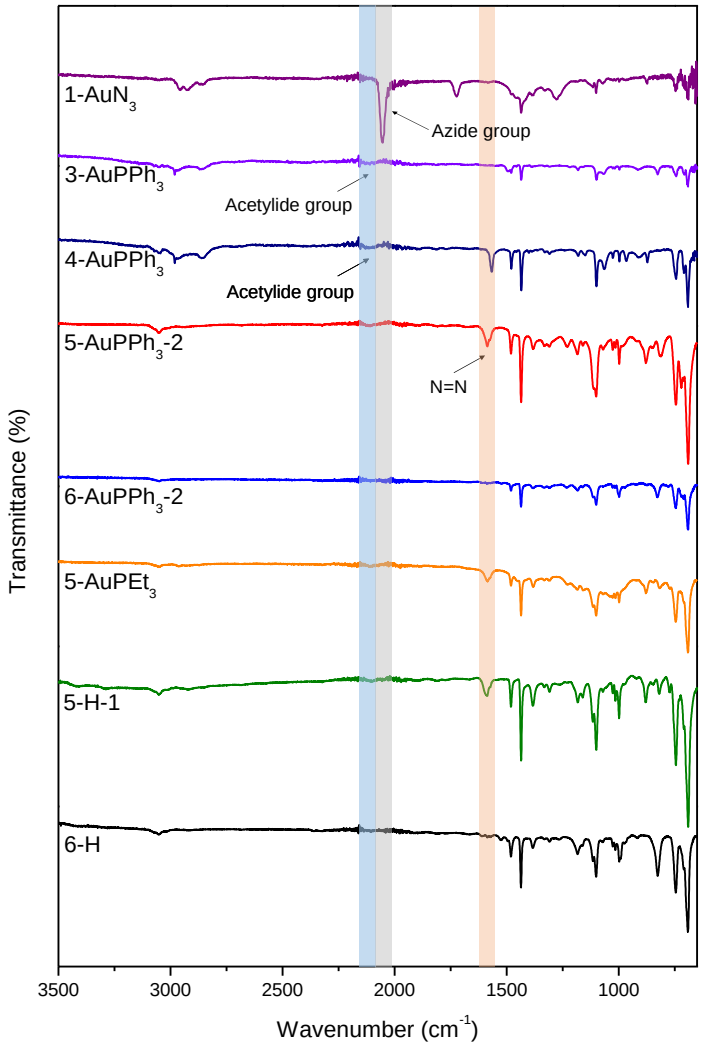

Figure S34. FTIR spectra of iClick network metallopolymers (**Table S3**, entry **5-AuPPh$_3$-2**, **6-AuPPh$_3$-2**, **5-AuPEt$_3$**, **5-H-1**, and **6-H**) in comparison with **1Au-N$_3$**, **3-AuPPh$_3$**, and **4-AuPPh$_3$**.

3.2 Solid-state CPMAS ^{13}C NMR spectra of iClick Network Metallopolymers Compared with Model Complexes

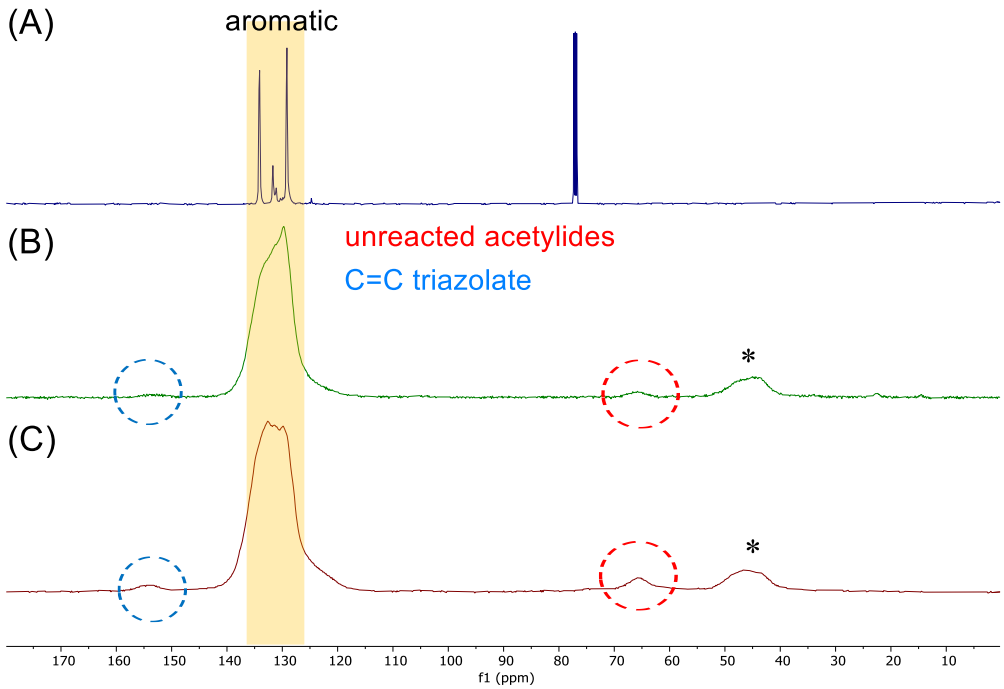

Figure S35. (A) The solution-phase $^{13}C\{^1H\}$ NMR of **7-AuPPh$_3$** ($CDCl_3$) in comparison with the solid-state ^{13}C NMR of (B) **7-AuPPh$_3$** and (C) **5-AuPPh$_3$-2** (* = spinning side bands (13 kHz)).

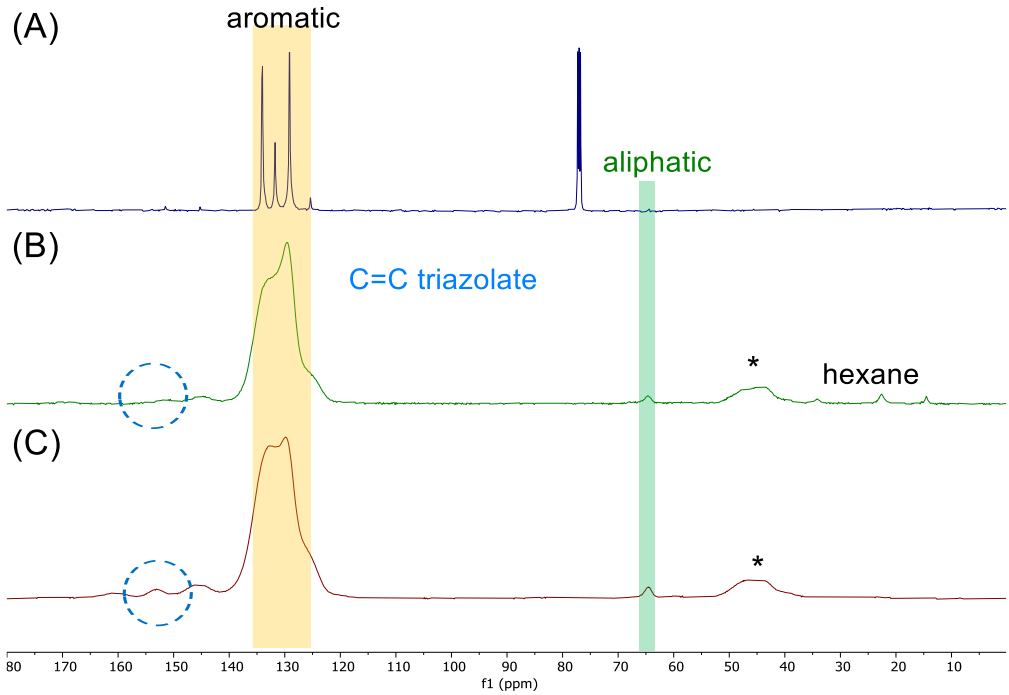

Figure S36. (A) The solution-phase $^{13}C\{^1H\}$ NMR of **8-AuPPh$_3$** ($CDCl_3$) in comparison with the solid-state ^{13}C NMR of (B) **8-AuPPh$_3$** and (C) **6-AuPPh$_3$-2** (* = spinning side bands (13 kHz)).

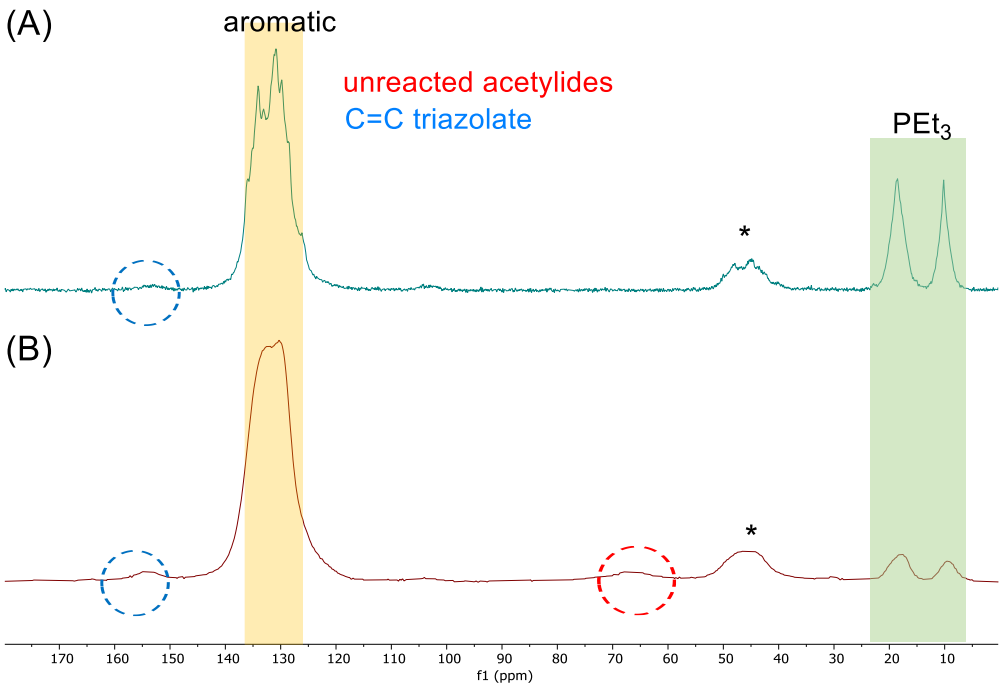

Figure S37. The solid-state ^{13}C NMR of (A) **7-AuPEt$_3$** and (B) **5-AuPEt$_3$** (* = spinning side bands (13 kHz)).

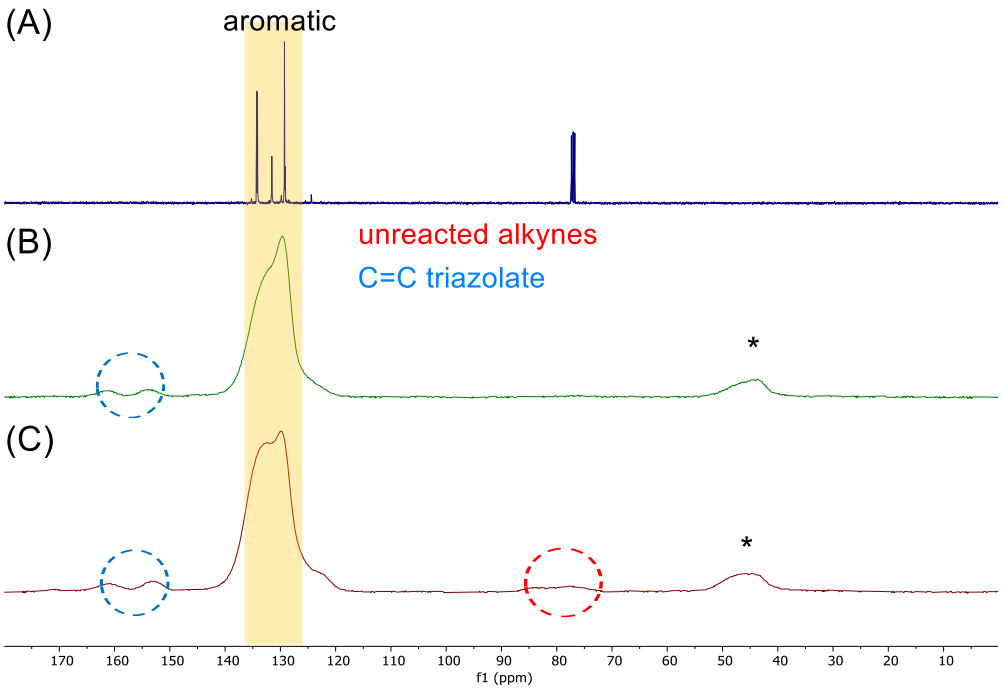

Figure S38. (A) The solution-phase $^{13}C\{^1H\}$ NMR of **7-H** ($CDCl_3$) in comparison with the solid-state ^{13}C NMR of (B) **7-H** and (C) **5-H-1** (* = spinning side bands (13 kHz)).

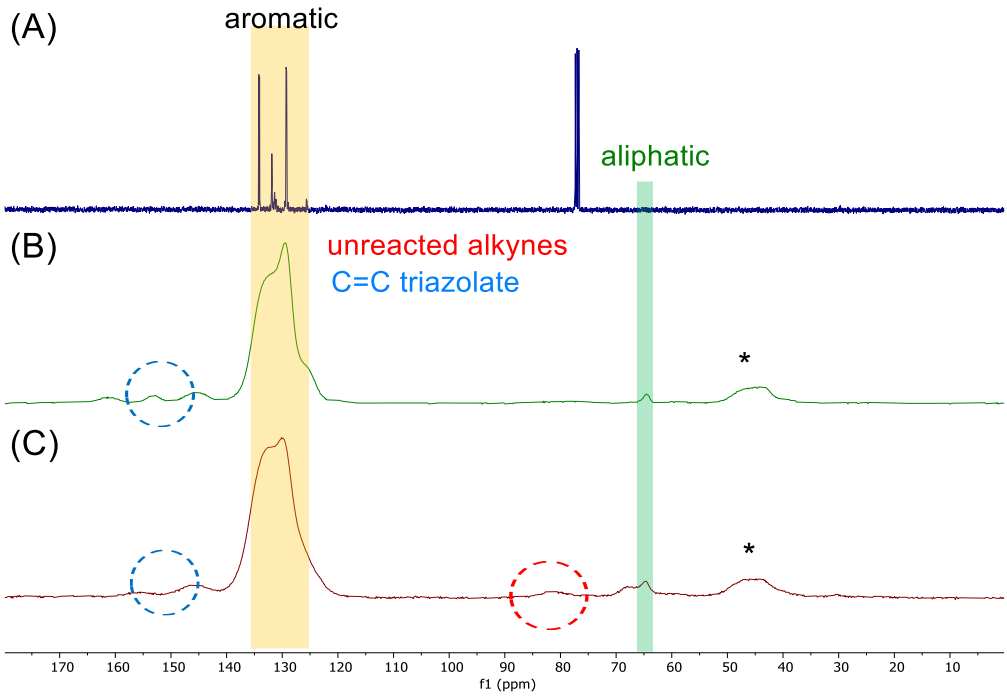

Figure S39. (A) The solution-phase $^{13}C\{^{1}H\}$ NMR of **8-H** ($CDCl_3$) in comparison with the solid-state ^{13}C NMR of (B) **8-H** and (C) **6-H** (* = spinning side bands (13 kHz)).

3.3 TGA profiles of iClick Network Metallopolymers

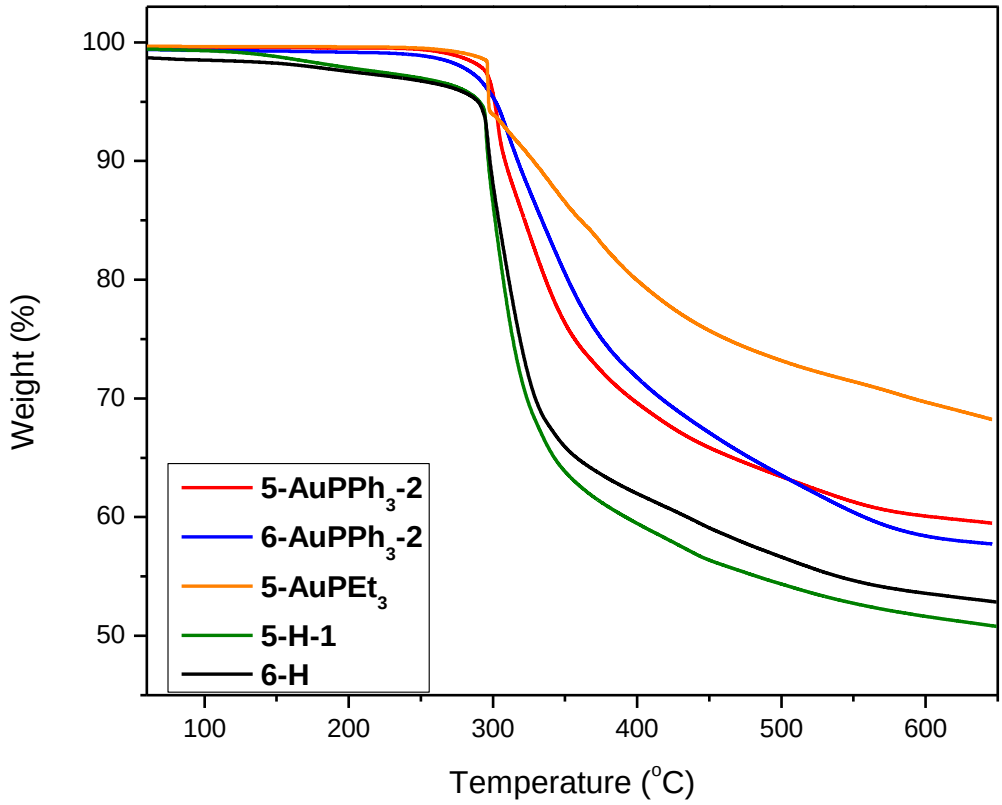

Figure S40. TGA curves of iClick network metallopolymers (**Table S3**, entry **5-AuPPh$_3$-2**, **6-AuPPh$_3$-2**, **5-AuPEt$_3$**, **5-H-1**, and **6-H**).

3.4 DSC spectra of iClick Network Metallopolymers

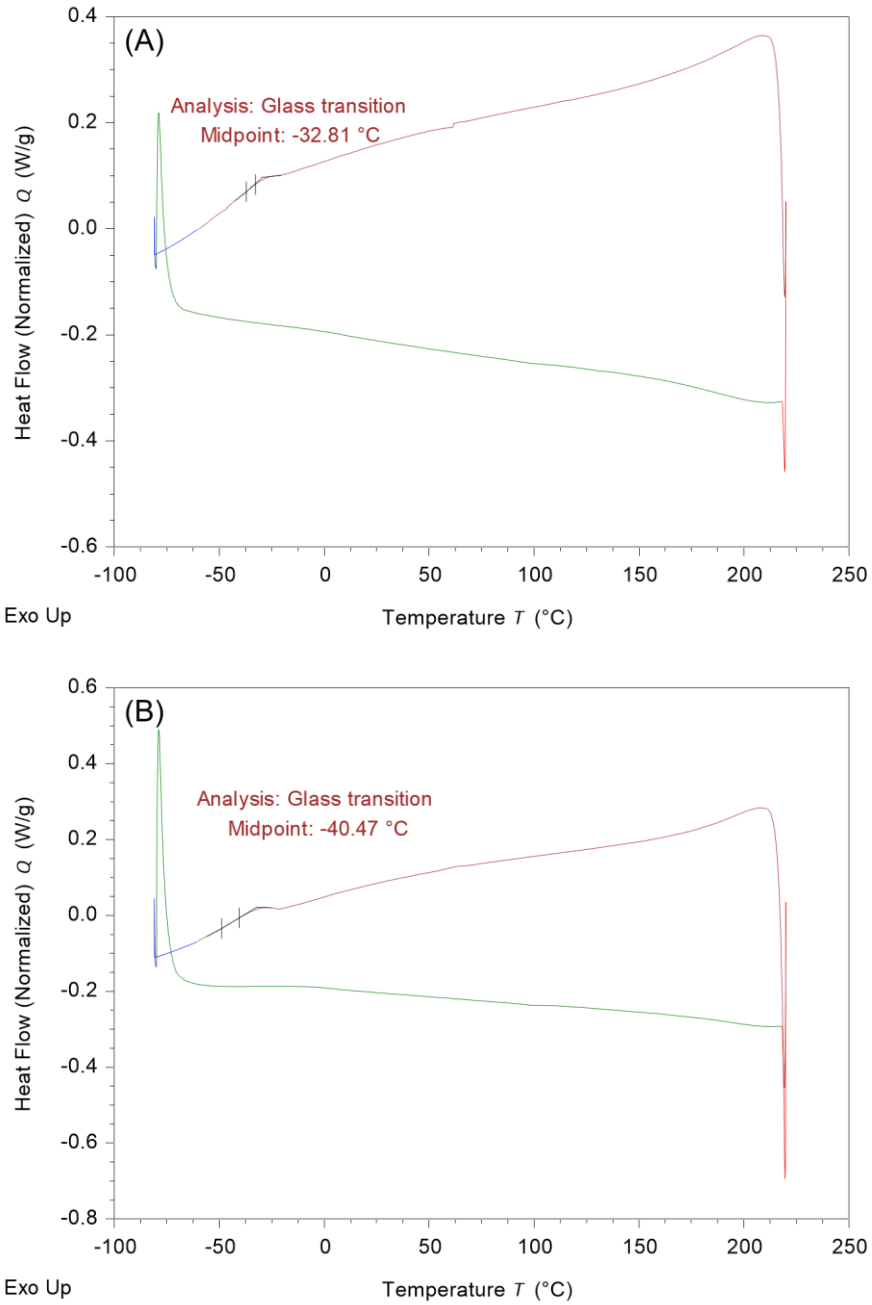

Figure S41. DSC curves of iClick network metallopolymers (A) **5-AuPPh$_3$-2** and (B) **6-AuPPh$_3$-2**.

3.5.1 N_2 Adsorption-desorption Isotherms of iClick Network Metallopolymers and Model Complex

Table S3. Effect of reaction time and reaction temperature on the pore properties of iClick network metallopolymers and model complex.

iClick metallopolymers	Entry	Reaction temp. (°C)	Reaction time (days)	Specific surface area[a] (m^2g^{-1})	Total pore volume[b] (cm^3g^{-1})	Yield (%)
5-AuPPh$_3$	**5-AuPPh$_3$-1**	rt	2	27	0.08	63
	5-AuPPh$_3$-2	50	6	94	0.19	76
	5-AuPPh$_3$-3	100	3	54	0.06	42
6-AuPPh$_3$	**6-AuPPh$_3$-1**	rt	2	44	0.13	94
	6-AuPPh$_3$-2	50	6	85	0.12	86
	6-AuPPh$_3$-3	100	3	47	0.08	40
5-AuPEt$_3$	**5-AuPEt$_3$**	50	6	30	0.07	95
5-H	**5-H-1**	50	1	28	0.04	83
	5-H-2	50	6	24	0.03	72
6-H	**6-H**	50	1	40	0.08	86
8-AuPPh$_3$	**8-AuPPh$_3$**	NA	NA	3	0.005	95

[a]BET specific surface area in the pressure range of 0.01–0.05 P/P_0 calculated using the BET model; [b]Total pore volume at P/P_0 = 0.95.

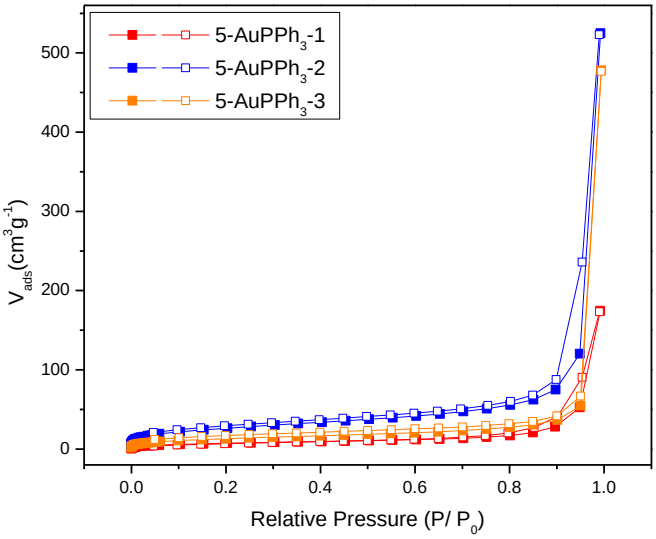

Figure S42. N_2 adsorption-desorption isotherms of iClick network metallopolymers **5-AuPPh$_3$** (**Table S3**, entry **5-AuPPh$_3$-1** to **5-AuPPh$_3$-3**).

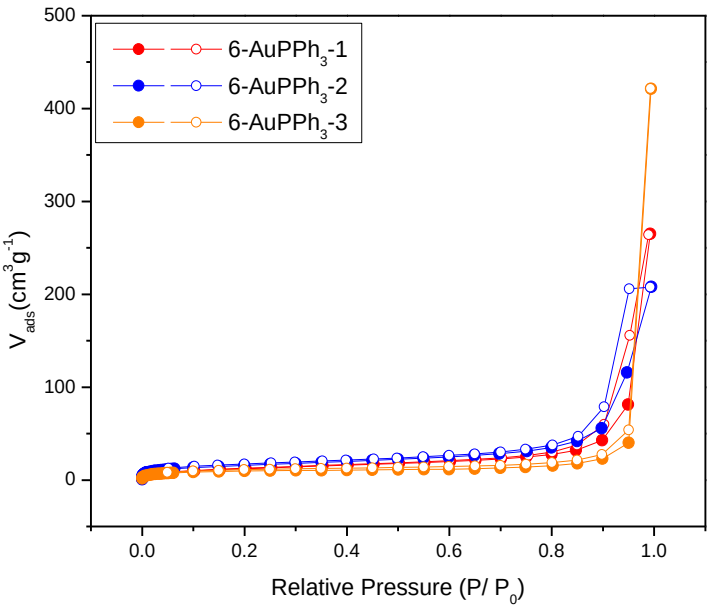

Figure S43. N_2 adsorption-desorption isotherms of iClick network metallopolymers **6-AuPPh$_3$** (**Table S3**, entry **6AuPPh$_3$-1** to **6-AuPPh$_3$-3**).

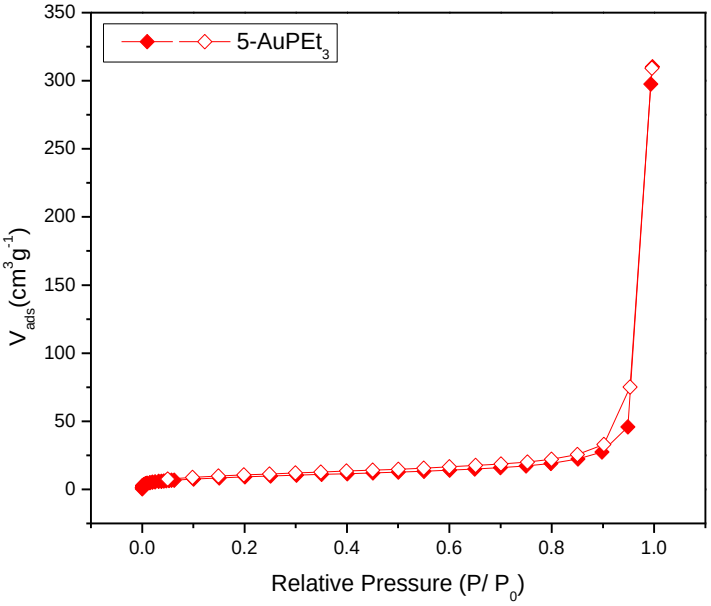

Figure S44. N_2 adsorption-desorption isotherms of iClick network metallopolymers **5-AuPEt$_3$** (**Table S3**, entry **5-AuPEt$_3$**).

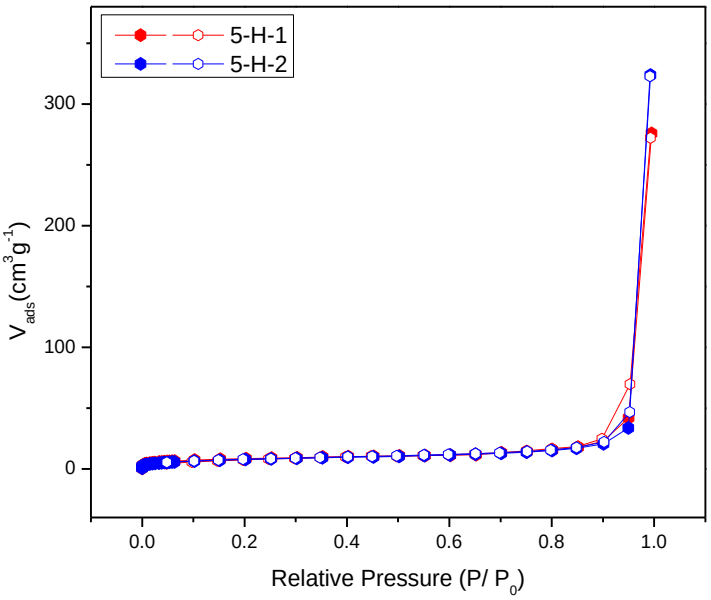

Figure S45. N_2 adsorption-desorption isotherms of iClick network metallopolymers **5-H** (**Table S3**, entry **5-H-1** and **5-H-2**).

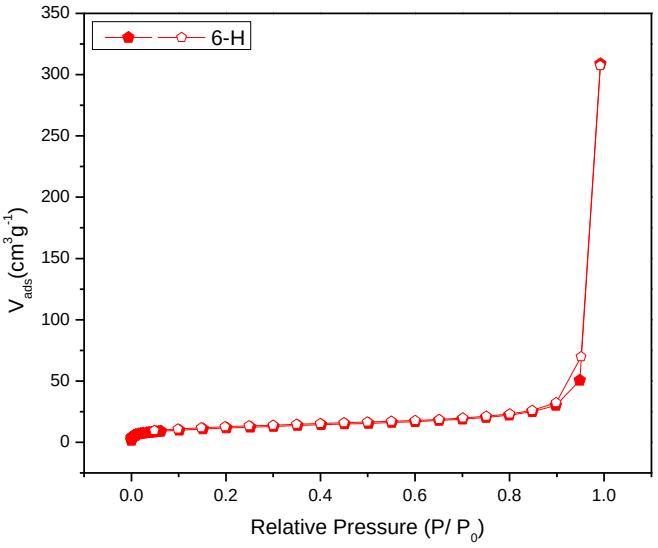

Figure S46. N_2 adsorption-desorption isotherms of iClick network metallopolymers **6-H** (**Table S3**, entry **6-H**).

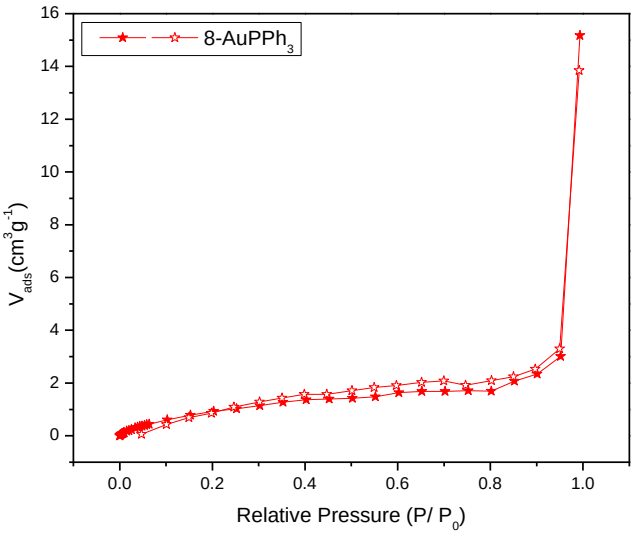

Figure S47. N_2 adsorption-desorption isotherms of model complex **8-AuPPh$_3$** (**Table S3**, entry **8-AuPPh$_3$**).

3.5.2 Improved Workup Procedure for Polymer **6-H**

The synthesis procedure was same as mentioned above in Section 2.2. The solution mixture was worked up by blowing gentle nitrogen flow to slowly evaporate the CH_2Cl_2 that was used as solvent.[8] When the solution was almost dried (still partially wet), solvent exchange with MeOH was applied. The process was repeated again with perfluorohexane (PFH),[9] and later slowly blowing nitrogen flow until all solvents evaporated to generate a white fluffy powder.[10]

The white powder was outgassed at a lower temperature. Instead of outgassing at 110 °C for 12 h, the powder was outgassed at 40 °C for 20 min and slowly increased at 1 °C/min to 100 °C and held for 5 h.[10]

The resulting surface area obtained was lower than the result indicated in Table S3.

The specific surface areas obtained were 25 m^2/g for powder that was solvent exchanged with MeOH and PFH and 29 m^2/g for powder that was solvent exchanged only with PFH.

3.6 CO_2 Adsorption-desorption Isotherms of iClick Network Metallopolymers

Table S4. CO_2 adsorption properties of iClick network metallopolymers

iClick metallopolymers	Entry	CO_2 uptake (298 K, mg g^{-1})	CO_2 uptake (273 K, mg g^{-1})
5-AuPPh$_3$	**5-AuPPh$_3$-2**	12.82	28.86
6-AuPPh$_3$	**6-Au PPh$_3$-2**	14.14	29.54
5-AuPEt$_3$	**5-AuPEt$_3$**	7.84	15.00
5-H	**5-H-1**	7.82	13.90
6-H	**6-H**	14.85	31.62

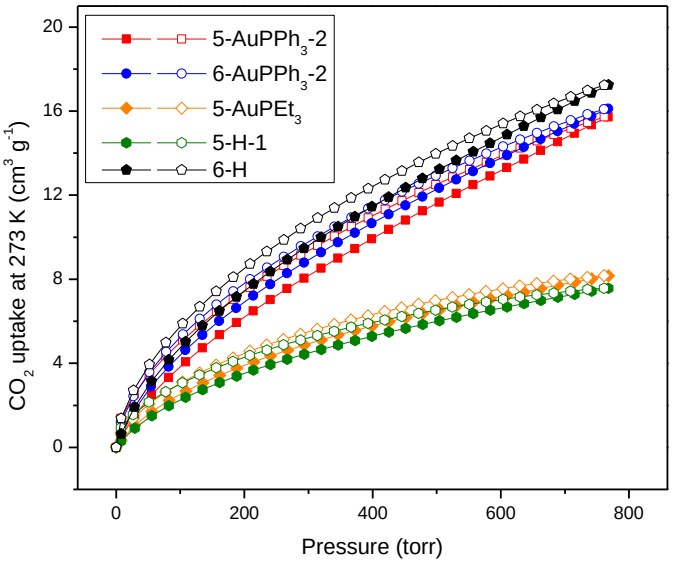

Figure S48. Carbon dioxide adsorption-desorption isotherm of iClick network metallopolymers at 273 K (**Table S3**, entry **5-AuPPh$_3$-2**, **6-AuPPh$_3$-2**, **5-AuPEt$_3$**, **5-H-1**, and **6-H**).

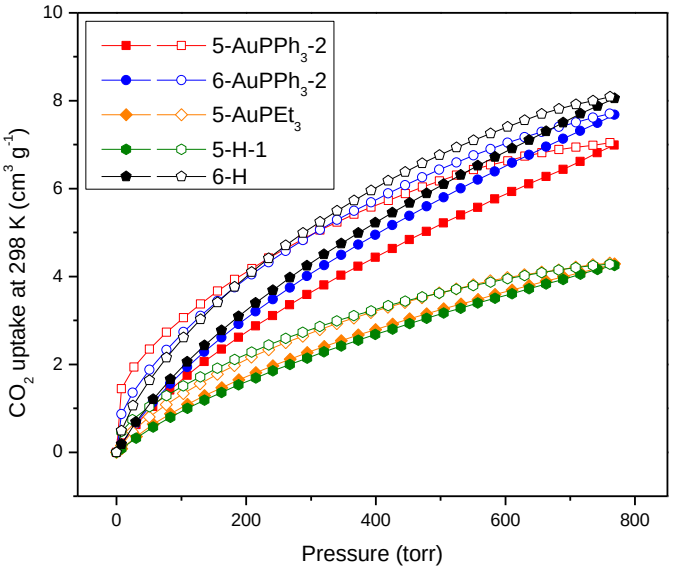

Figure S49. Carbon dioxide adsorption-desorption isotherm of iClick network metallopolymers at 298 K (**Table S3**, entry **5-AuPPh$_3$-2**, **6-AuPPh$_3$-2**, **5-AuPEt$_3$**, **5-H-1**, and **6-H**).

3.7 TEM and STEM images of iClick Network Metallopolymer

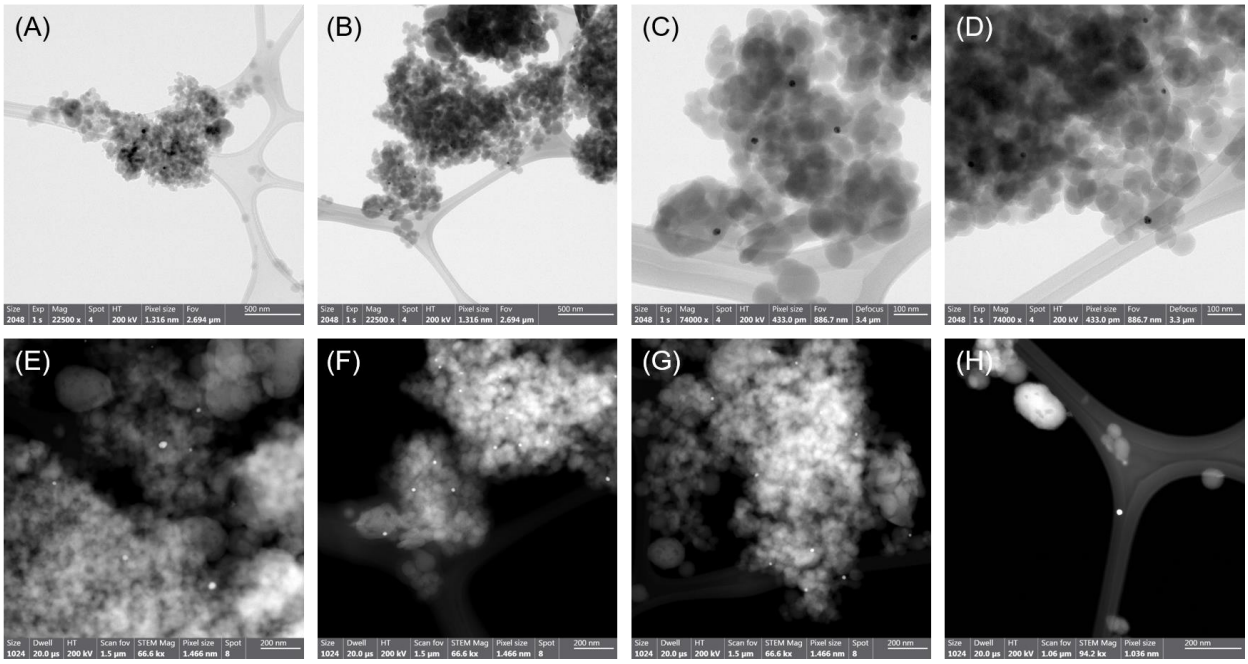

Figure S50. TEM images of the iClick network metallopolymer **6-AuPPh$_3$-2** at 2 different scales (A) and (B) 500 nm, (C) and (D) 100 nm; STEM images of **6-AuPPh$_3$-2** at 200 nm (E)-(H).

3.8 STEM EDS spectra of iClick Network Metallopolymer

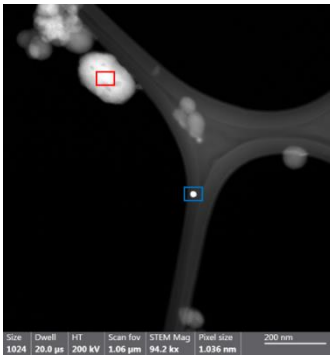

Figure S49. (H) The STEM image of polymer **6-AuPPh$_3$-2** for EDS analysis. The red square is the area analyzed as network polymers, and the blue square is the area assigned for Au nanoparticles in the EDS analysis.

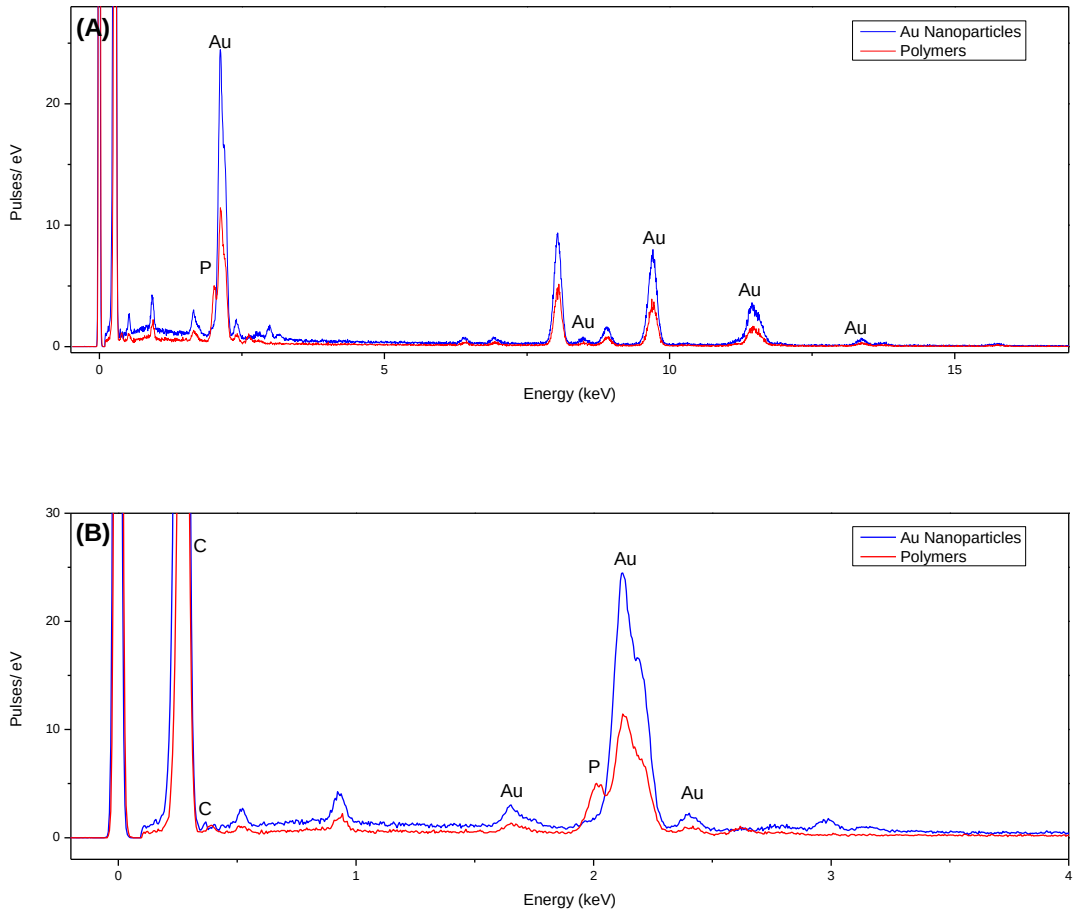

Figure S51. STEM EDS spectrum of the iClick network metallopolymer **6-AuPPh$_3$-2**. (A) full spectrum, (B) blow-up spectrum from 0-4 keV.

3.9 SEM and BSE SEM images of iClick Network Metallopolymer

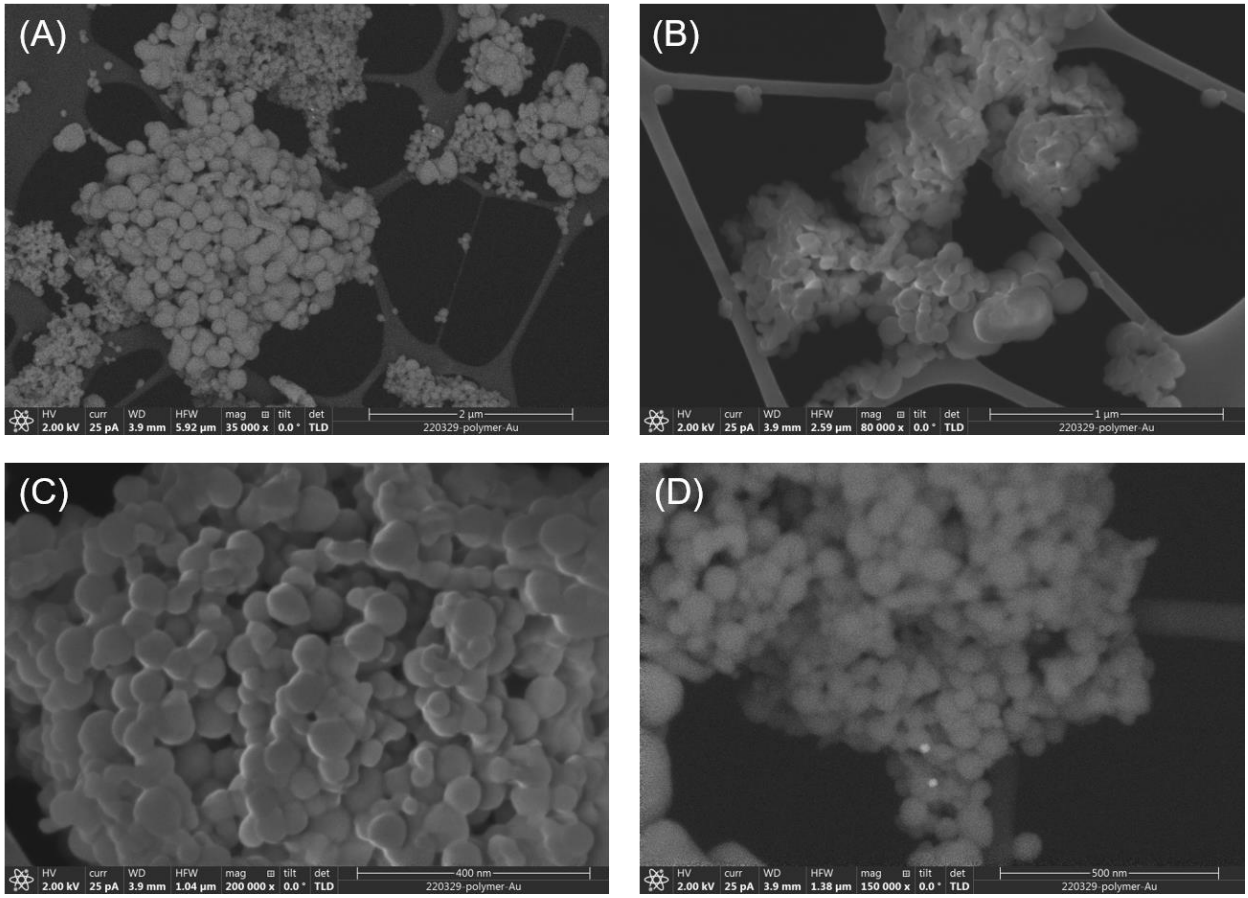

Figure S52. SEM images of the iClick network metallopolymer **6-AuPPh$_3$-2** at 3 different scales (A) 2 μm, (B) 1 μm, (C) 400 nm. (D) BSE SEM image of **6-AuPPh$_3$-2** at 500 nm.

3.10 PXRD of iClick Network Metallopolymers

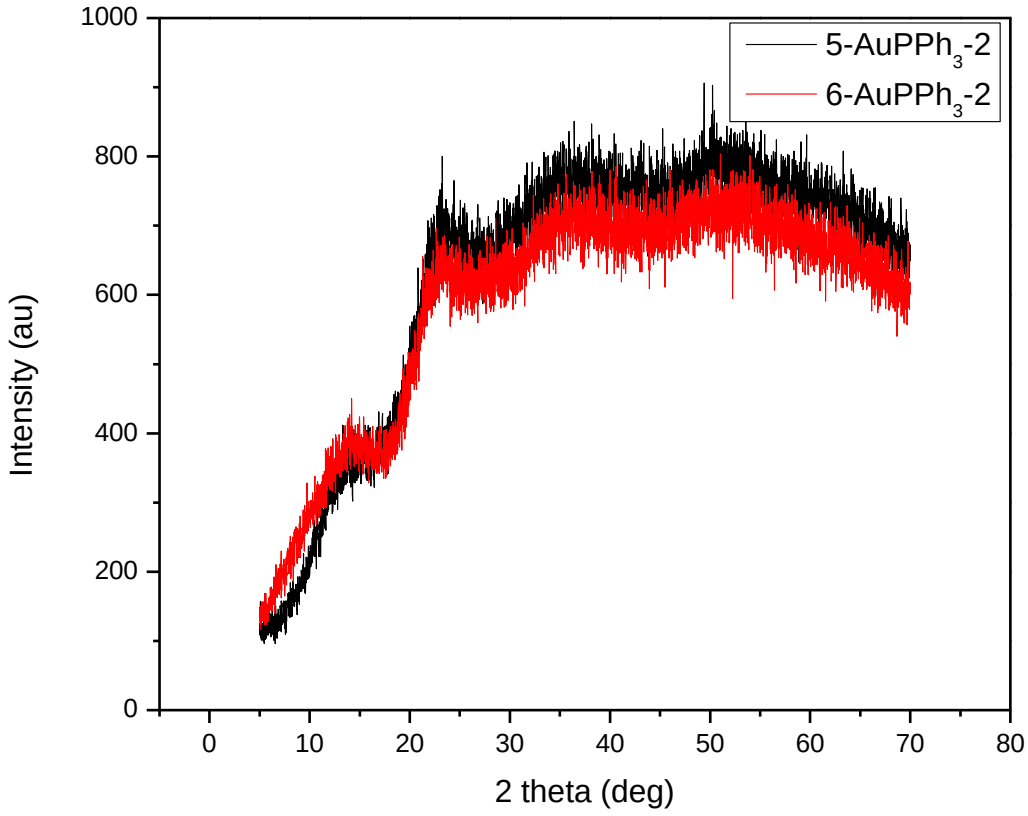

Figure S53. PXRD data of the iClick network metallopolymers **5-AuPPh$_3$-2** and **6-AuPPh$_3$-2**.

4. References

1 H. C. Kolb, M. G. Finn and K. B. Sharpless, *Angew. Chem. Int. Ed.*, 2001, **40**, 2004–2021.

2 J. Cámara, O. Crespo, M. C. Gimeno, I. O. Koshevoy, A. Laguna, I. Ospino, E. S. Smirnova and S. P. Tunik, *Dalton Trans.*, 2012, **41**, 13891–13898.

3 P. Pandey, O. K. Farha, A. M. Spokoyny, C. A. Mirkin, M. G. Kanatzidis, J. T. Hupp and S. T. Nguyen, *J. Mater. Chem.*, 2011, **21**, 1700–1703.

4 J. Luo, X. Liu, M. Ma, J. Tang and F. Huang, *Eur. Polym. J.*, 2020, **129**, 109628.

5 I. R. Whittall, M. G. Humphrey, S. Houbrechts, J. Maes, A. Persoons, S. Schmid and D. C. R. Hockless, *J. Organomet. Chem.*, 1997, **544**, 277–283.

6 G. M. Sheldrick, *Acta Cryst.*, 2015, **C71**, 3–8.

7 A. L. Spek, *Acta Crystallogr. Sect. C Struct. Chem.*, 2015, **71**, 9–18.

8 C. H. Feriante, S. Jhulki, A. M. Evans, R. R. Dasari, K. Slicker, W. R. Dichtel, S. R. Marder, C. H. Feriante, S. Jhulki, R. R. Dasari, K. Slicker, S. R. Marder, A. M. Evans and W. R. Dichtel, *Adv. Mater.*, 2020, **32**, 1905776.

9 D. Zhu and R. Verduzco, *ACS Appl. Mater. Interfaces*, 2020, **12**, 33121–33127.

10 E. Vitaku and W. R. Dichtel, *J. Am. Chem. Soc.*, 2017, **139**, 12911–12914.